Santa Clara University
Scholar Commons

Spring 2023

Robotic Arm Extrusion End Effector

Nicholas Viamin

David Blouin

Savannah Hunt

Nico Figueroa

SANTA CLARA UNIVERSITY

Department of Mechanical Engineering

Department of Electrical and Computer Engineering

I HEREBY RECOMMEND THAT THE THESIS PREPARED
UNDER MY SUPERVISION BY

Nicolas Viamin, David Blouin, Savannah Hunt, Nico Figueroa

ENTITLED

Robotic Arm Extrusion End Effector

BE ACCEPTED IN PARTIAL FULFILLMENT OF THE REQUIREMENTS FOR THE
DEGREE OF

BACHELOR OF SCIENCE
IN
MECHANICAL ENGINEERING
AND
ELECTRICAL AND COMPUTER ENGINEERING

<table>
<tr><td></td><td>6/14/2023</td></tr>
<tr><td>Mechanical Engineering Thesis Advisor</td><td>date</td></tr>
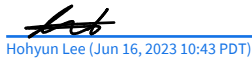<tr><td></td><td>6/14/2023</td></tr>
<tr><td>Electrical and Computer Engineering Thesis Advisor</td><td>date</td></tr>
<tr><td>Hohyun Lee (Jun 16, 2023 10:43 PDT)</td><td>06/16/23</td></tr>
<tr><td>Mechanical Engineering Department Chair</td><td>date</td></tr>
<tr><td></td><td>06/16/23</td></tr>
<tr><td>Electrical and Computer Engineering Department Chair</td><td>date</td></tr>
</table>

Thesis_Robotic Arm Extrusion End Effector

Final Audit Report   2023-06-16

Created:	2023-06-16
By:	Darcy Yaley (dyaley@scu.edu)
Status:	Signed
Transaction ID:	CBJCHBCAABAALIyKwfFFBEkPXKGo6AcyVdV3ttGP3H51

"Thesis_Robotic Arm Extrusion End Effector" History

Document created by Darcy Yaley (dyaley@scu.edu)
2023-06-16 - 3:40:57 PM GMT

Document emailed to hlee@scu.edu for signature
2023-06-16 - 3:42:00 PM GMT

Email viewed by hlee@scu.edu
2023-06-16 - 5:43:21 PM GMT

Signer hlee@scu.edu entered name at signing as Hohyun Lee
2023-06-16 - 5:43:44 PM GMT

Document e-signed by Hohyun Lee (hlee@scu.edu)
Signature Date: 2023-06-16 - 5:43:46 PM GMT - Time Source: server

Document emailed to Shoba Krishnan (skrishnan@scu.edu) for signature
2023-06-16 - 5:43:47 PM GMT

Email viewed by Shoba Krishnan (skrishnan@scu.edu)
2023-06-16 - 6:22:28 PM GMT

Document e-signed by Shoba Krishnan (skrishnan@scu.edu)
Signature Date: 2023-06-16 - 9:17:46 PM GMT - Time Source: server

Agreement completed.
2023-06-16 - 9:17:46 PM GMT

Robotic Arm Extrusion End Effector

By

Nicholas Viamin, David Blouin, Savannah Hunt, Nico Figueroa

SENIOR DESIGN PROJECT REPORT

Submitted to
the Department of Mechanical Engineering
and
Department of Electrical Engineering

of

SANTA CLARA UNIVERSITY

in Partial Fulfillment of the Requirements
for the degree of
Bachelor of Science in Mechanical Engineering
and the degree of
Bachelor of Science in Electrical Engineering
and the degree of
Bachelor of Science in Electrical and Computer Engineering

Santa Clara, California

Spring 2023

Robotic Arm Extrusion End Effector

David Blouin, Nick Viamin, Savannah Hunt, & Nico Figueroa

Departments of
Electrical Engineering & Mechanical Engineering

Santa Clara University

2023

Abstract

This senior design project aims to enhance the capabilities of the Rotrics AIO Desktop Arm (Dexarm) by designing and implementing an extrusion device capable of smooth and consistent extrusion for 3D printing applications. The project focused on ensuring safety, affordability, and ease-of-use for users, while achieving precise control over the extrusion process. Various mechanical and electrical components were carefully selected to ensure compatibility with the Dexarm and to provide optimal performance. To maintain safety, extensive testing and risk assessments were conducted to minimize any potential hazards associated with the extrusion process. To achieve smooth and consistent extrusion, precise control mechanisms were developed. The successful implementation of the extrusion device was validated through the 3D printing of a small bowl using classroom clay. The device demonstrated its capability to accurately deposit the clay material layer by layer, resulting in a well-defined and functional object.

Acknowledgements

We would firstly like to thank our advisors, Dr. Andy Wolfe from the Electrical and Computer Engineering department and Dr. Pete Woytowitz from the Mechanical Engineering department.

Additionally, we would like to give special thanks to Rodney Broome for his endless support throughout our project as well as the entire Engineering School for the financial assistance that made this project possible.

Table of Contents

List of Figures

List of Tables

List of Equations

Chapter 1: Introduction

Our Robotic Arm Extrusion End Effector strives to introduce a robotic arm end effector that could extrude highly viscous materials in order to overcome the shortcomings of conventional extrusion techniques for such materials. Our initial research brought to light how conventional extrusion techniques are labor and money-intensive, which causes delays in the production of the intended product. Despite the fact that autonomous extruders are available on the market, including the WASP and the DeltaBots 3D Potterbots, referenced in Reference 9 and 10 respectively, their exorbitant price makes it less practical for budget-conscious hobbyists and small manufacturers to use them. Our team set out to provide a relatively inexpensive and practical solution that would enable for the continuous extrusion and molding of highly viscous materials after realizing the influence on a variety of industries, including industry, hobbyists, and education.

Shown in the figure below, is our completed device and a bowl that was printed using our device for future reference throughout this paper.
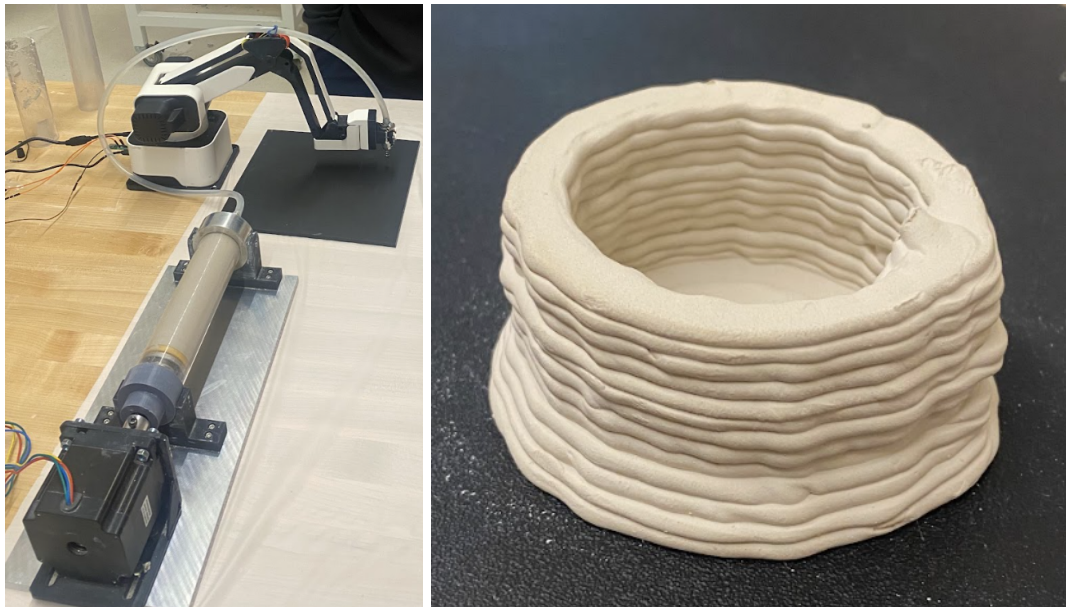
Figure 1: Completed Device [Left] and a Printed Bowl [Right]

1.1 Choosing This Project

When selecting this project, there were numerous factors that led our team to consider designing and building a robotic arm extrusion end effector. During the beginning of our research, we were intrigued by the possibilities in the world of 3D printing. Our team looked into the idea of extruding various materials such as cookie dough, frosting, and clay. After weighing in our

different options regarding our intended material to extrude, we decided that it would be the most practical to extrude a ceramic material like clay due to the high viscosity of the material as well as the various applications it could be used for. Our Robotic Arm Extrusion End Effector offers a multitude of compelling incentives for those who are interested. It provides a renewed opportunity to contribute to technological innovation and development. It enables individuals to explore new 3D printing possibilities through pushing the boundaries of conventional extrusion methods. The development of a robotic arm end effector capable of extruding extremely viscous materials paves the way for novel manufacturing techniques as well as positions participants at the cutting edge of research and development.

Second, our project addresses a critical need in the manufacturing industry for cost and time efficiency. Traditional extrusion techniques frequently rely on manual labor which requires a significant investment in regards to time and resources. Through the development of an automated and precise extrusion system, this project seeks to streamline the manufacturing process and reduce labor-related expenses. This aspect is particularly appealing to manufacturers seeking to optimize their production processes and increase their competitive advantage.

In addition, partaking in this project is consistent with the larger objective of promoting sustainable manufacturing practices. Individuals can contribute to reducing waste and environmental impact by investigating alternative extrusion techniques and optimizing material usage. This area appeals to those who are conscientious about environmental sustainability and are looking for methods to apply their skills to create a more sustainable future.

Taking on the Robotic Arm Extrusion End Effector project provides the opportunity to promote innovation, enhance both cost and time efficiency, and contribute to environmentally responsible manufacturing practices. Individuals seeking to have a significant impact in the fields of robotics and additive manufacturing will find this initiative appealing for the preceding reasons.

1.2 Project Goal

The ultimate objective of the Robotic Arm Extrusion End Effector project was to create a system for extruding extremely viscous materials with both affordability and precision in mind. In other words, the goal of the project is to develop a robotic arm end effector capable of extruding highly viscous materials with a high level of precision, consistency, and speed while maintaining a reasonable budget.

By achieving this objective, our extruder has the intention of expanding the field of additive manufacturing. The development of a dependable and automated extrusion system creates new opportunities for the manufacturing of complex structures, customized products, and advanced

prototypes. The foremost objective is to allow for the creation of 3D-printed objects with a broad variety of materials, including those that are traditionally challenging to extrude.

In addition, our project aims to improve the overall productivity and cost-effectiveness of the manufacturing process. By automating the extrusion procedure, this extruder device intends to reduce reliance on manual labor, reduce material waste, and maximize resource utilization. This contributes towards enhanced manufacturing, industry productivity and competitiveness.

Another goal of our project is to promote sustainability by investigating alternative extrusion techniques and maximizing material utilization. This includes seeking to reduce material waste and the environmental impacts that are associated with traditional extrusion techniques by creating a system that can efficiently manage highly viscous materials with minimal waste. For this reason, one of our main objectives is to promote sustainable manufacturing practices and contribute to a more environmentally conscious approach to production.

The long-term goal of the Robotic Arm Extrusion End Effector project is to have a positive impact on the manufacturing industry by pushing the boundaries of additive manufacturing, improving efficiency, expanding application possibilities, and promoting sustainable practices. Given that there was sufficient wasting of material during our testing, it is apparent that we would have to aim to make our extruder more efficient with extruding the clay. In other words, the amount of clay we input into the device should be nearly the same as the amount of clay outputted. This would ensure minimal waste of material and ultimately promote a more sustainable manufacturing.

1.3 Ethical Considerations

Our Robotic Arm Extrusion End Effector project takes a variety of ethical concerns into consideration. First, our project needs to guarantee the safety of everyone who uses the device, which may include researchers, technicians, and end-users. This entails implementing robust safety protocols and mechanisms to ensure the prevention of accidents and injuries throughout the development, testing, and operation of the robotic arm. In order to prioritize a positive impact on society and minimize the project's potential hazards, ethical guidelines must be followed. This project must take the ethical ramifications of automation into consideration along with its potential effects on employment. The introduction of an advanced and automated extrusion system may result in the reduction and even the elimination of jobs in certain industries. It is vital to evaluate the potential repercussions and formulate strategies to mitigate the negative effects on workers. This may entail retraining programs, providing assistance to affected individuals, and investigating new employment opportunities promoted by technological advancement.

In addition, our team addressed the issues of accessibility and equity. It is essential to ensure that the benefits and advancements related to our extruder device are accessible to a broad range of communities and individuals. It is necessary to take measures when marketing this product to take into account the technological divide between various communities to prevent the escalation of existing social disparities. In designing and implementing the robotic arm extrusion system, it is necessary to consider affordability, availability, and usability. Environmental sustainability and the responsible management of resources are additional ethical factors to consider. Our initiative should aim to reduce material waste, promote recycling/the reuse of material, and investigate extrusion materials that are friendly to the environment. In addition, the materials that are used to make up the device should be analyzed to ensure that they can be disposed of or reused under the circumstance that the device breaks, while also taking into account other factors such as energy consumption, and ecological footprint of the extrusion materials. Moreover, this project must comply with the legal frameworks pertaining to intellectual property. Considerate and ethical research/development entails preserving intellectual property rights along with acquiring informed consent for the collection and use of data. Our research must ensure that we do not infringe upon the copyrights of other similar products that may have patented designs.

In assessing how we achieved these goals, we were able to stay true to our intentions in most aspects of our considerations. We believe that we made our system simple enough for people outside of the profession of engineering to be able to learn how to use while also providing a powerful interface for 3D printing. The only consideration where we felt we fell short was our excessive use of materials in testing our design. Naturally clay is a material that requires a good deal of cleaning before and after use so we had to use a lot of paper towels and other single use materials to clean our workspace.

Chapter 2: Overall System Integration

In order to be able to complete a project which integrates electrical, mechanical, materials, and computer engineering, the delegation of tasks as well as the steps to completion needed to be properly and thoughtfully defined. In this chapter of our thesis, we will talk about the overall structure of the system we set out to create, the way we structured our team as a result, and the overall process of designing the said system.

2.1 System Overview

To fully understand the team structure and the chosen design for this project, it is vital to understand the constraints that were present from the start. First, we were kindly lent a Rotrics robotic arm by one of our advisors, Dr. Wolfe. This arm came with its own program for 3D printing, used by one of its many attachments. This gave us an excellent platform upon which to write and generate our own 3D printing designs. The robot arm, while it had many benefits, did have its own set of limitations. It could only hold up to 500 grams, for example. Due to the heavy nature of the materials, the design would need to conform to allow the weight of the material and material pressurizer to be independent of the robot arm. The software, while it also came with many benefits, had drawbacks as well. Moving the pressure chamber motor in sync with the robot arm was a task that required much research and coding.
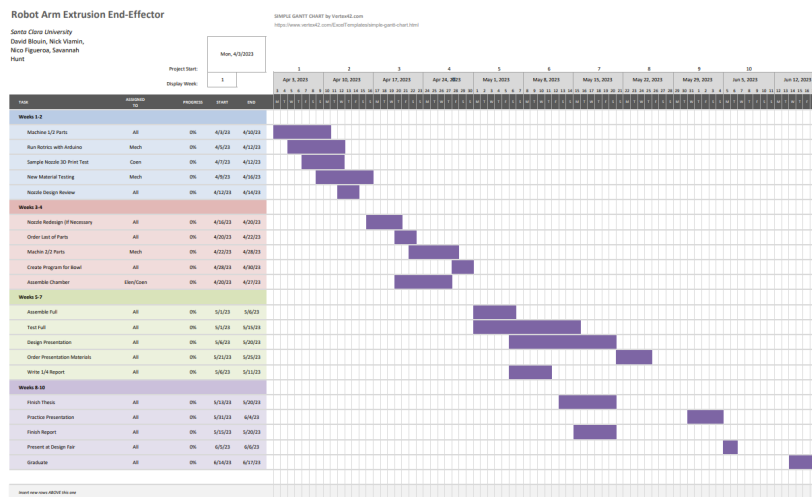
Figure 2: Spring Quarter Gantt Chart

Shown in figure 2, is our initial Gantt chart for our spring quarter project plans, we stayed relatively close to our original timeline despite the numerous challenges which we were extremely happy with.

2.2 Team Structure

To address these concerns, our team, consisting of two mechanical engineers, one electrical engineer, and one computer and electrical engineer, developed an outline complete with goals and dates these goals should be completed, as seen in Figure 2. The task of designing the main structure of the system was given to the mechanical engineers along with the evaluation and testing of the used material. The electrical hardware and software was given to the electrical engineers, the software more specifically allotted to the computer and electrical engineer.

2.3 Design Process

The reason that our goal of creating a system which extrudes highly viscous materials is such a difficult task to achieve lies in the nature of these thick materials. Not only are they viscous, but oftentimes, they have a non-negligible amount of elasticity, greatly differing their behavior under high pressures and impulse impacts. They are also very heavy, causing them to be difficult to maneuver. These reasons indicated the need for a very strong system that could implement immense loads of pressure very gradually. We also understood that, because of the weight of the material, it is unlikely that the robot arm we were given, the rotrics, could support the full system if mounted on the end effector. Through evaluation such as this, we were able to determine the steps that were vital to our design process. First, we needed to run calculations using the density and viscosity of the material used in order to determine the torque necessary to extrude the material up to a given velocity. We also understood that running Ansys simulations would be helpful in determining the amount of pressure the mechanical system would experience. Next, we realized that we needed to keep the pressure chamber on the side of the robot arm to ensure a precise print. With regards to electrical, knowing what motor we would need would allow the proper motor driver and power supply to be chosen. Finally, understanding the material properties would allow us to alter the print speed and motor speed accordingly.

Chapter 3: Pressure Chamber

The pressure chamber is one of the most important aspects of this project which is why we spent a significant amount of our allotted time both designing and building this section. Through various design iterations using the CAD software SolidWorks, the following design was reached, seen in Figure 3.
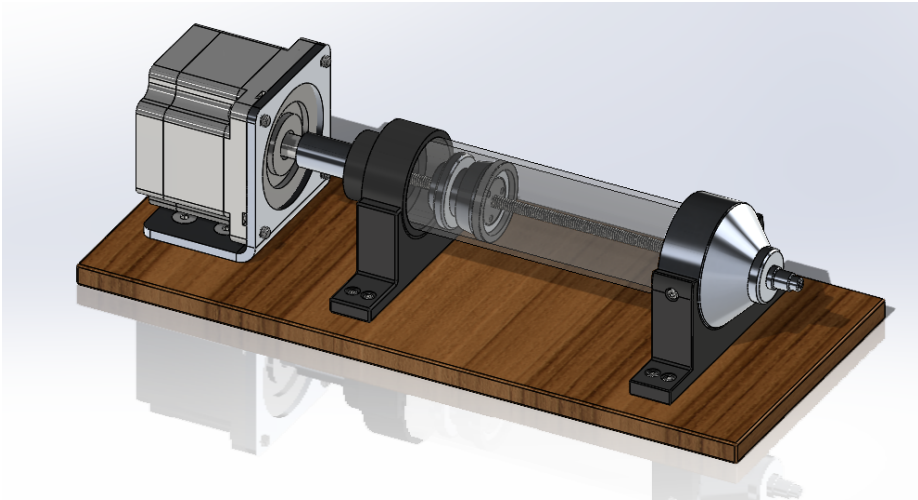
Figure 3: Pressure Chamber CAD Design

3.1 Mechanical Design Process

Throughout the course of our Fall quarter, we came up with multiple pressure chamber designs. Figure 4 shows one of our first design iterations.
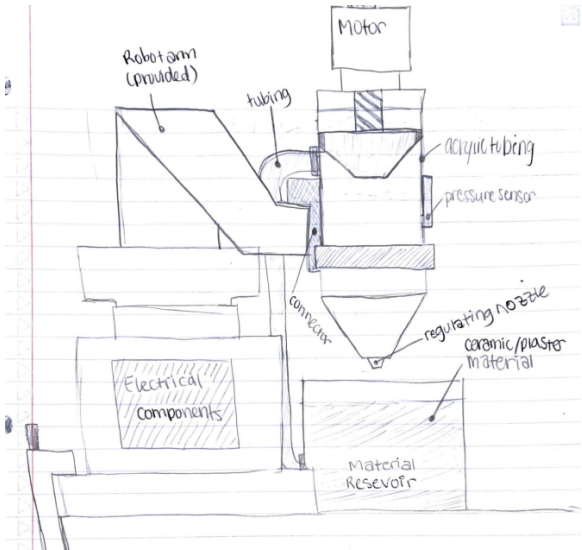
Figure 4: Early Design Drawing

While this method of mounting the pressure chamber on the robot arm is used by some of our competing companies, the design does not fit our constraints since our robot arm does not have the capacity to operate well under the necessary amount of weight. Because of this, we began investigating other designs such as the one seen in Figure 5 below.
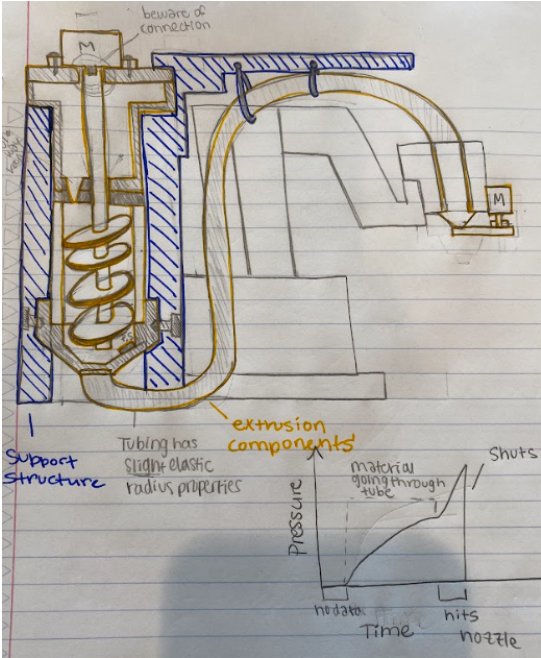
Figure 5: Archimedes Screw Design Drawing

This design implements an archimedes screw to pressurize the material. We even went so far as to create a CAD model made on SolidWorks for this system, seen in Figure 6.
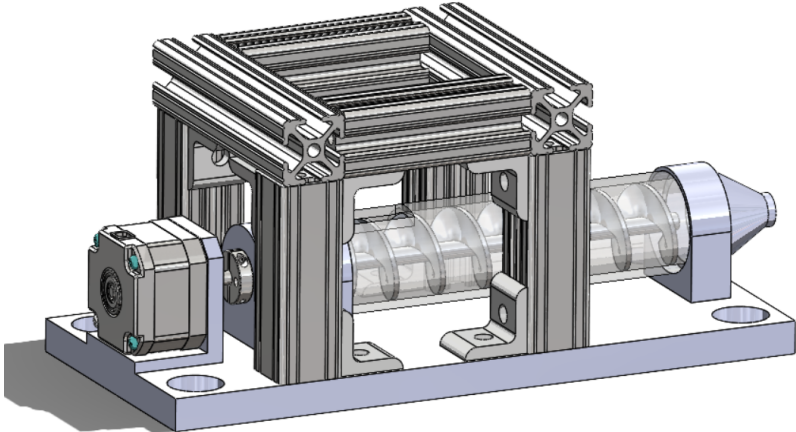
Figure 6: Archimedes Screw Design CAD

After much consideration, and after referencing an archimedes screw design journal, Reference 8 and Appendix I, we decided that the pressure given to the material with this type of system would not be enough to move our highly viscous material through the narrow piping. For this reason, we began investigating the use of a high-power press. Figure 7, pictured below, shows our first concept drawing using the press method. As one can see in this drawing, the idea was to initially include a refill inlet to allow the system to refill mid-print. At the time, there was the worry that the system would not hold enough material to complete an entire print.
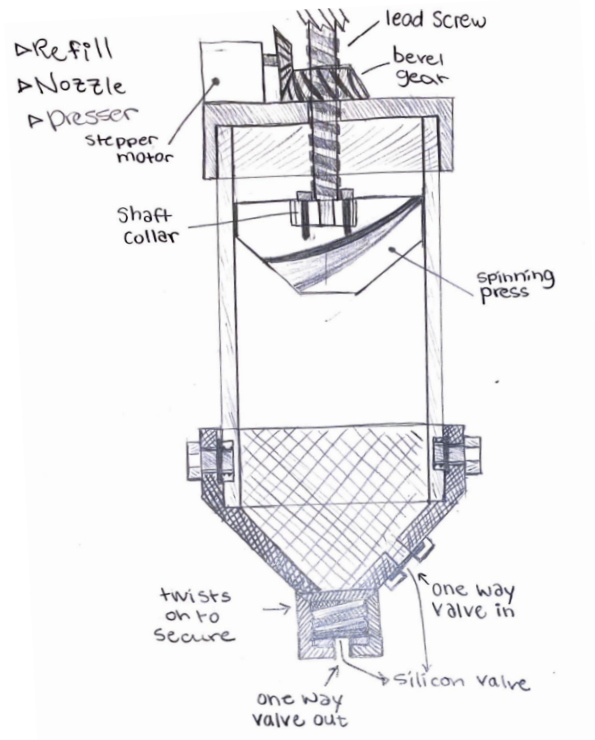
Figure 7: Preliminary Press Design Drawing

Despite this concern, our team decided to proceed first without a refill valve for simplicity. We also determined through volumetric calculations, found in the calculations section, that the material in the chamber would be enough to print a bowl, which was our goal for this project. After approximately three weeks of CAD work using SolidWorks, we finally produced our official pressure chamber design, seen in Figure 8.
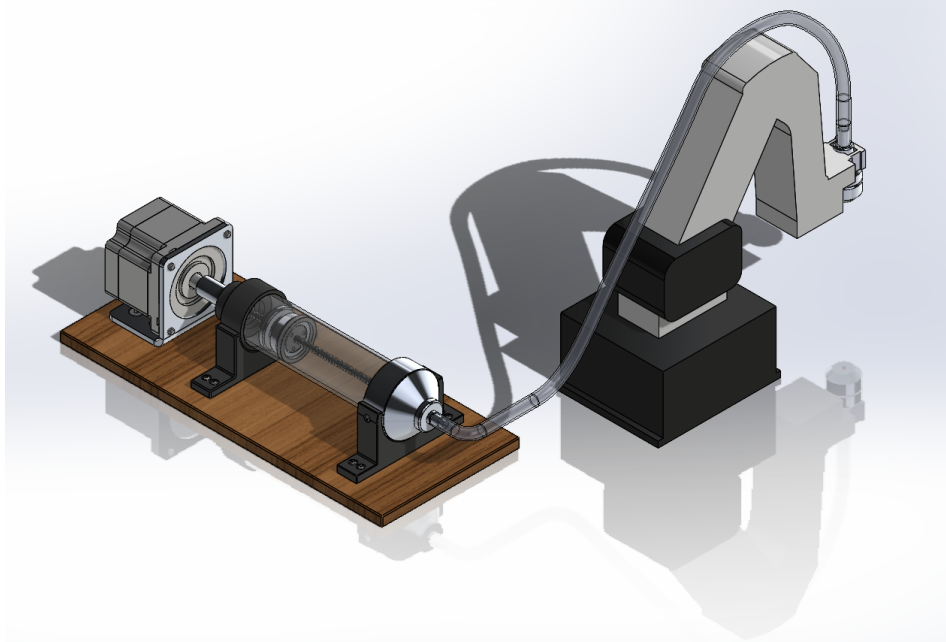
Figure 8: Final Full System SolidWorks Assembly

This design utilized a NEMA 34 motor, the derivations of which can be found in the calculations section of this thesis paper, to turn a ¼"-20 steel lead screw, which in turn caused the lead nut holding the press to move in the linear direction. This then pressurized the material held within the 2" polycarbonate cylinder, forcing it to navigate into the smaller tubing, which connected to the nozzle. All of this was to be mounted on an aluminum ½" thick base plate.
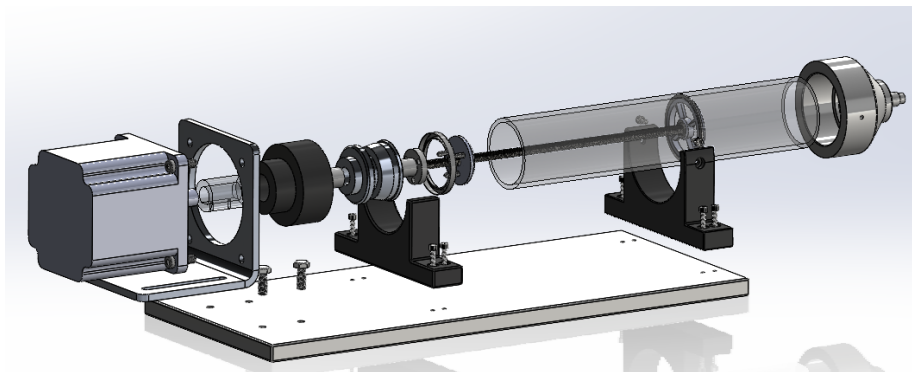
Figure 9: Pressure Chamber Exploded View

Once we had the design finalized, we ordered the necessary parts from McMaster Carr, Amazon Prime, and TAP Plastics. With these items ordered, we moved on to the fabrication of the remaining parts.

3.2 Fabrication Steps

There were ten total parts that needed fabrication or alteration. These parts and the fabrication necessary can be seen in Table 1 below.

Table 1: Part Fabrication Chart

Part	Material	Fabrication Type
Large Nozzle Connector	Aluminum	Lathing plus Milling
Base Plate	Aluminum	Milling
Press	Aluminum	Lathing plus Milling
Motor Coupler	Aluminum	Lathing
Pressure Chamber Mounts (QTY 2)	PLA and PETG	3D Printed
Press Protecting Piece	PLA	3D Printed
Lead Screw	Steel	Lathe
Back End Piece	PLA	3D Print
Lead Screw Stabilizer	PLA	3D Print

For the parts which needed to be 3D printed, we utilized the maker's lab's 3D printers. As for the metal parts, these needed to be machined and we did so in the college machine shop run by Professor Broome. For the large nozzle connector, made out of aluminum, we machined much of this part on the lathe, pictured in Figure 10, but completed the final touches on the mill.

Figure 10: Machining Large Nozzle Using Lathe

This part was especially difficult since it has tapers both on the outside as well as on the inside of the piece. This allows the nozzle to funnel the material into a smaller diameter with the least amount of losses. The final part can be seen attached to its mount below, Figure 11.

Figure 11: Finished Large Nozzle in Mount

The next part we machined was the press. This part had complex geometry because it needed to fit exactly into the seal which we ordered on McMaster. The isometric sectioned view shows this complex taper, circled in red, in Figure 12.

Figure 12: Section View of McMaster Seal

With intensive lathing and then eventual milling, the part was completed, fitting nicely into the seal ring, as intended. Figure 13 shows the press, seal, lead nut, and lead screw assembled and pressed into the polycarbonate tubing.

Figure 13: Assembled Press and Lead Screw

After creating the press, we moved on to milling the base plate. This was one of our simpler pieces as it only required taking the plate down to size, drilling holes, and tapping these holes. The second to last piece that needed machining was the motor coupler, this part needed to be able to rotate with the motor shaft and connect to the shaft coupler we ordered from McMaster. This shaft coupler then connected with the lead screw which, in turn, allowed the lead screw to move as one with the motor shaft, shown in Figure 14.
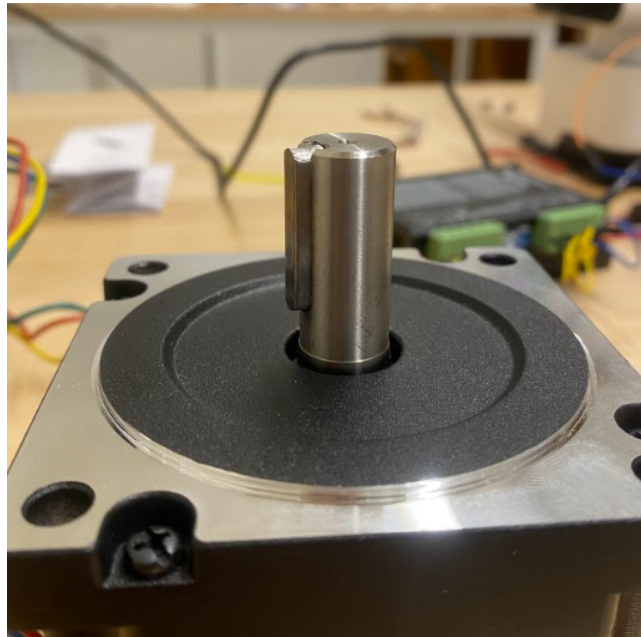
Figure 14: NEMA 34 Axle

This part, the CAD model shown in Figure 15, took various iterations due to the complexity of the motor shaft shape. In the end, we decided to create a hole which was the diameter of the motor shaft, remove the shaft key, and use this groove as a spot to secure two screws that go through the side of the motor coupler. This allowed the motor to turn the motor coupler as it rotated.
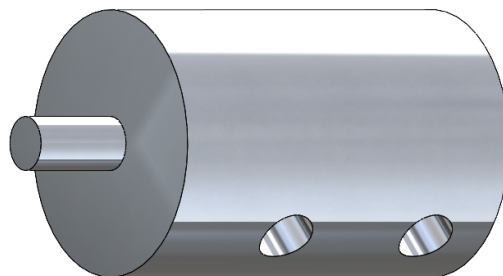
Figure 15: Motor Coupler SolidWorks Model

The final part to machine was actually a part ordered from McMaster. This was our ¼"-20 Steel Lead Screw. The ends, in order to fit into the proper shaft coupler and end stabilizer, needed to be taken down to the proper diameter, the drawings of which show this in Figure 16.
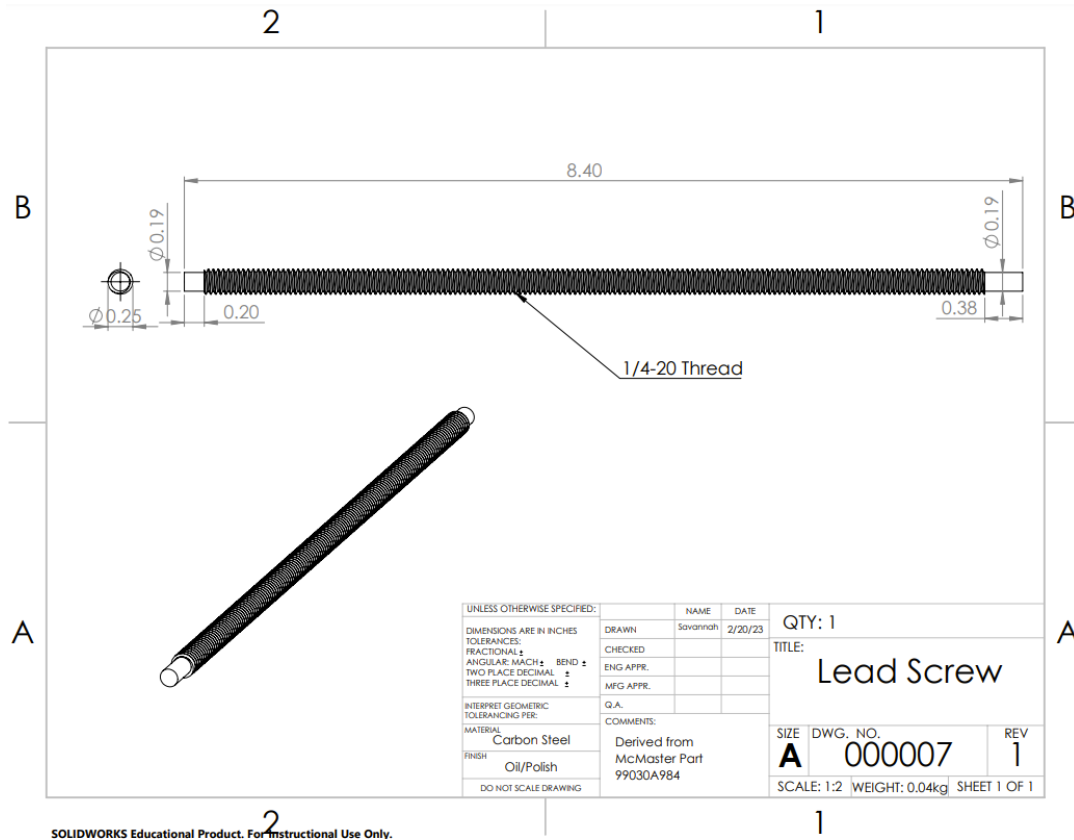
Figure 16: Lead Screw SolidWorks Drawing

The reason we decided to do this instead of making the shaft coupler and end stabilizer holes larger was to create a flat, even surface upon which these two parts could grip. This reduced possible vibrational interference and inconsistent frictional forces.

Figure 17: Machining Lead Screw with Lathe

This part was, thus, lathed down to size and deburred to restore the threads, as shown in Figure 17.

Once all of our parts were printed, machined, and ordered, we moved on to the assembly process.

3.3 Assembly & Future Improvements

The final step to the design process of the pressure chamber was the assembly of the parts. This went relatively quickly since the design was intended to be relatively simple to assemble. Our group recognized the need for DFM as well as DFA while in the CAD stages of this project. Figure 18 shows the final pretrial, assembled pressure chamber.
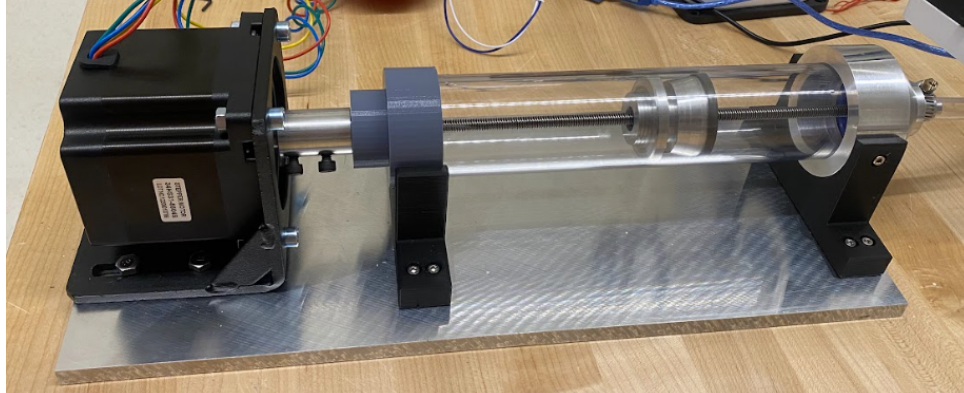
Figure 18: Full Assembly of Pressure Chamber

Future improvements might include using the force of gravity to our advantage by turning the entire pressure chamber vertically with the large nozzle facing down. This might pose other issues, though, so the change might require the redesign of multiple parts of this system. This added force of gravity might also be insignificant compared to the force of the motor, rendering this design unnecessary. Where change must occur to improve this project is in the securement of the front large nozzle to the base. This would reduce losses due to leakage and minimize overall system failure due to fatigue fractures.

Chapter 4: Dispensing Nozzle

The other key section of this system is the dispensing nozzle. During the process of designing this section, there were many iterations and changes made due to fabrication and time constraints. These will be covered in the next few subsections.

4.1 Mechanical Design Process

It is important to understand first what we wanted to achieve with the dispensing nozzle when evaluating its design process. It needed to be able to dispense the material at a diameter which allowed for precise and accurate prints. With this in mind, it was also vital to design a nozzle that was not too small in diameter for the type of materials we would be working with. In an ideal scenario, we also wanted the nozzle to cut off material instantaneously when the motor spun back slightly, relieving pressure on the nozzle. Therefore, in our first design iteration, we played around with the idea of using a small stepper motor to cut off the material when the arm was moving locations/not printing, as shown in the drawing in Figure 19.
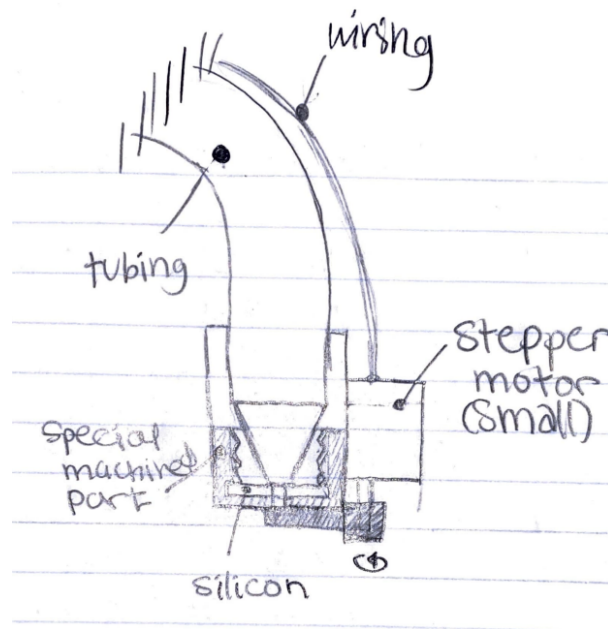
Figure 19: Early Nozzle Design Drawing

While this design may have worked, it likely would have been difficult to fine-tune the system into creating an accurate cut off when needed. It also adds another level of complexity to the coding of the system. In addition to this, the added weight of the motor might have created unwanted momentum forces, causing the print to be less precise. Therefore, we decided to move on to other ideas. The next concept we came up with was to include a small sheet of thin silicon

with a 3 mm slit cut in the center. This silicon piece would lie inside the nozzle, acting as a backpressure that, when fluid pressure dipped below a certain value, would overtake the forward motion of the fluid, effectively closing the slit. This would make it so that no more material would flow and the print would be essentially 'cut'. The CAD model of this design can be seen in Figure 20.

Figure 20: Nozzle SolidWorks Assembly

The section view is seen in Figure 21 and shows the internal design of this nozzle version. The silicon pad, in orange, is placed directly under the top piece of the nozzle. Directly under is the cap which screws on, creating a tight seal.

Figure 21: Section View of CAD Nozzle

While this concept may have worked well, due to time constraints, we were not able to fabricate or test this design.

4.2 Fabrication Steps

Instead of machining these parts with the little time we had left, Professor Broome offered us a great solution for the meantime. He gave us two hose couplers, pictured in Figure 22 and referenced in reference 4.

Figure 22: Hose Couplers[1]

They are made of stainless steel, detach into two parts for easy cleaning, and fit on our end effector excellently, see Figure 23. Also visible in Figure 23 is that the top of the hose coupler is attached to the tubing using a pipe clamp. This created a strong seal between the highly pressurized tubing and the nozzle.

---

[1] "MC1604 1/4" Hose Barb Non-Valved Body", page 1.
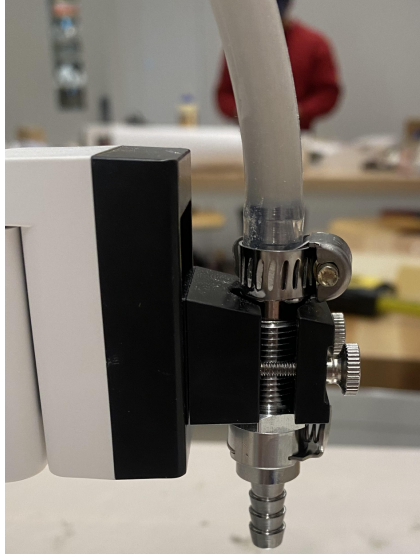
Figure 23: Final Assembled Nozzle

While the outlet hole was larger than our initial design, this proved to be an effective size for the printing of a bowl.

4.3 Future Improvements

While this nozzle did work for our testing, it does not have a cut off feature like our second design. This caused there to be lots of extra material dispensed pre- and post-print. Our suggestion would be for future teams to include a silicon piece or some other cutting method to ensure a cleaner print. This will also allow for the printing of more complex designs.

Chapter 5: System Analysis

In the process of designing this system, we needed to understand the forces acting upon the various parts. To do so, we worked with Ansys, reference 1, to create simulations and conduct various material testing methods. Using the results of these simulations and tests, we calculated the torque levels necessary for our main motor and better understood what materials each part should be made of.

5.1 Ansys Simulation

In order to run proper Ansys Simulations, we first broke our total system into three subsystems, analyzing the fluid dynamics in each. The first system was our main pressure chamber. This was to be a 2 inch outer diameter tube with a wall thickness of ⅛ inches.

Due to not knowing the exact viscosity of the material we will be using, we ran the simulations with a material that has similar viscosity to the expected viscosity of our material: molasses. It has a viscosity of 10,000 CPI[2] and a density of 1360 kg/m^3.

We put an inlet velocity of 0.5 m/s. We also added a backpressure of 3,144.65 Pa, simulating a backwards force of 5 Newtons. The simulation setup can be seen in Figure 24.
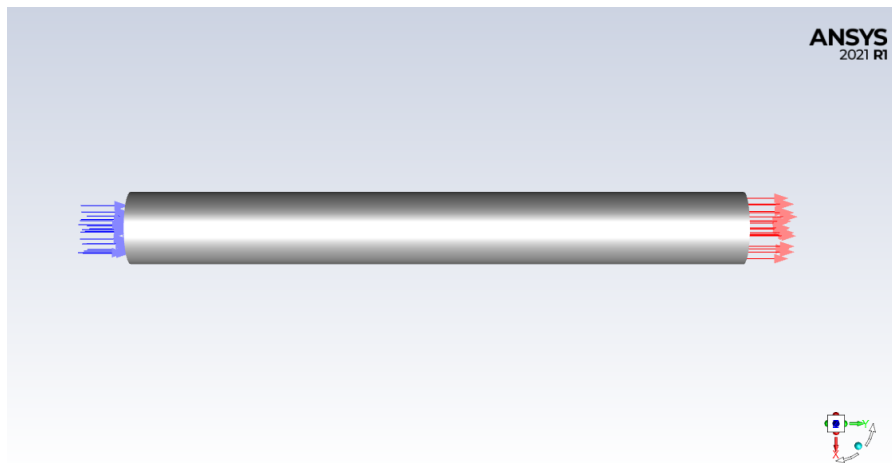
Figure 24: Ansys Flow Setup in Pressure Chamber

From Figure 25, one can see that the outlet velocity peaks at the center of the tube outlet. This makes sense since the drag force from the walls causes the center of the fluid to increase in speed, compensating for the reduced speed of the fluid at the walls. The fluid speed reaches up to

---

[2] "Viscosity Scale", *Smooth On.*

double the inlet velocity at this center, as expected. This is because the boundary wall boundary conditions on the top and bottom of the fluid and no resistance in the center.
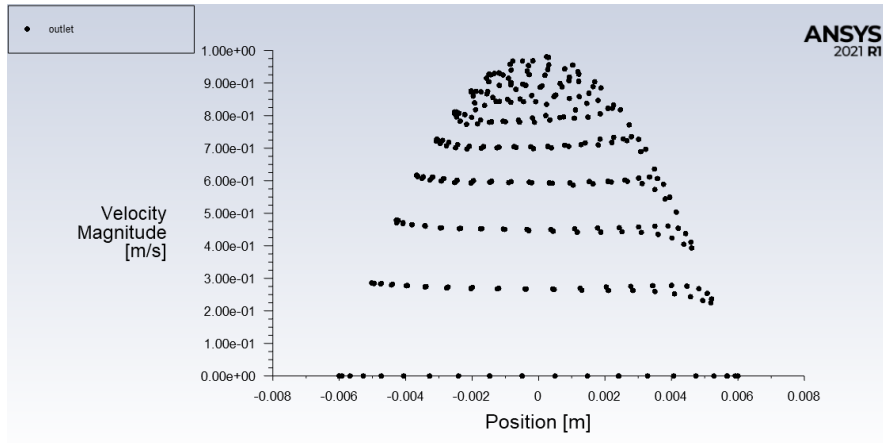
Figure 25: Exit Velocity Graph Pressure Chamber

Figure 26 again confirms this point, this time at the exit of the long tubing, as it shows the velocity gradient of the outlet, the highest speed being centralized and the speeds decreasing as you move towards the cylinder wall. One can also see the lighter colors, indicating a slower velocity, along the cylinder walls.
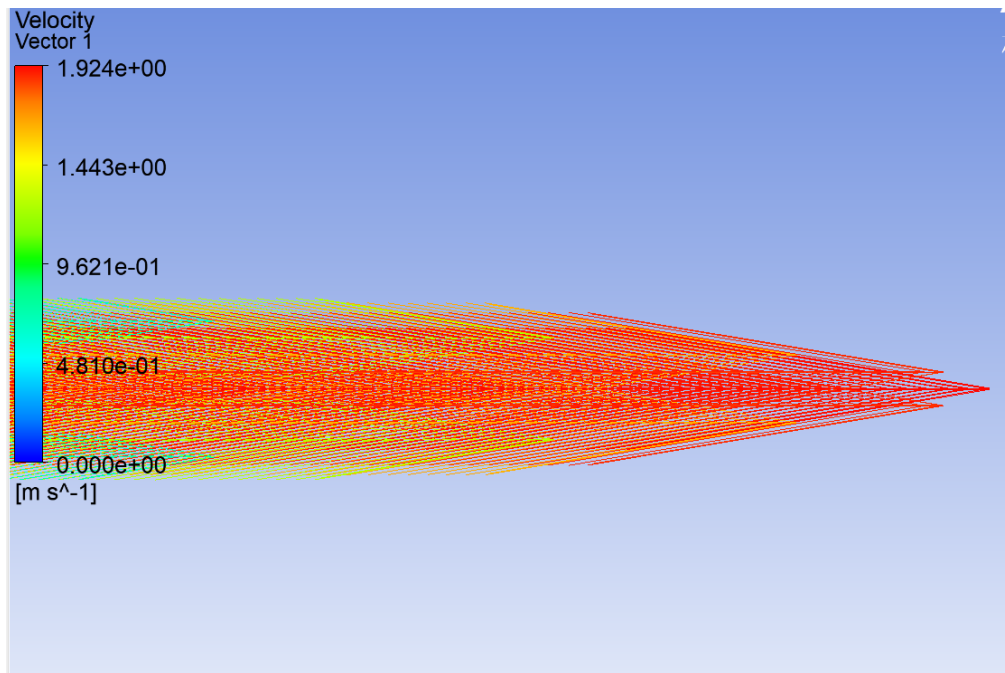
Figure 26: Velocity Vectors of Long Tubing

The next section we ran Ansys on was the long thin tube leading from the pressure chamber to the dispensing nozzle. The pressure gradient of this section can be seen in Figure 27. The length of the tube was set to 2 feet and the diameter, a ½ inch.
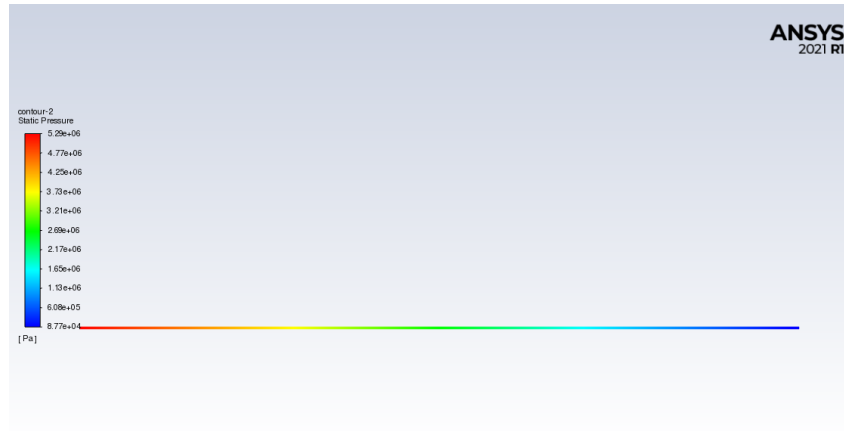
Figure 27: Pressure Gradient in Long Tubing

The pressure gradient shows that the most pressure will be experienced at the inlet, where the large nozzle connects with the narrow tubing. We would later find this to be true in our various trials. With an inlet velocity of 1 m/s, the highest outlet velocity was found to be 2 m/s, again doubling.

The final section we simulated was that of the dispensing nozzle. Figure 28 displays the velocity gradient with an inlet velocity of 2 m/s and was found to exit the narrow end of the nozzle at 32 m/s, a 16 fold increase.
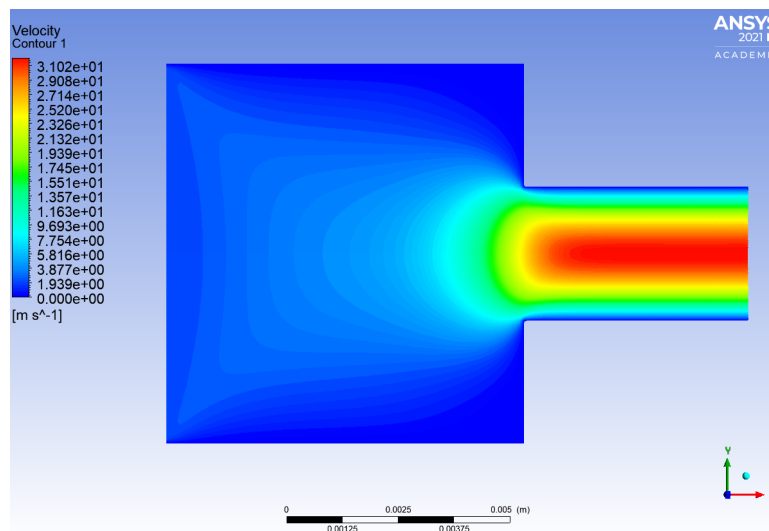
Figure 28: Velocity Gradient in Nozzle

This significant increase was something we needed to keep in mind when programming the speed of the press in the pressure chamber.

5.2 Material Testing

Selecting the proper material to extrude through our system was an extensive process. Before we purchased any material for testing we first had to determine the parameters we were aiming for. The goal for our system was to extrude highly viscous materials so we began our search by testing powdered ceramic material that had an adjustable viscosity depending on the amount of water we added. The mixture we created with the ceramic powder had a viscosity that we thought would be good enough to extrude through the system, but the drying time was too short for our use. Several times material hardened in test polycarbonate tubing which made the material impossible to work with, and it also ruined some of the tubing we were going to use for the pressure chamber. We determined that the ceramic powder was not a good material for this purpose so we pivoted to clay.

The clay material we chose is also known as "classroom clay." We purchased around 5.2 kg of this material and mixed it with water until we obtained a clay/water mixture with the viscosity we desired. We chose this style of clay because it provided us with workability of our mixture, and if properly mixed it is easily compressible, smooth, and it dries into a solid. After some ratio testing, we determined that a ratio of 100 ml of water for every 1 kg of clay was the best mixture for our system. This ratio provided us with a good consistency for printing and allowed the material to hold up each subsequent layer. In order to get the most consistent mixture possible, we obtained a drill mixer attachment for a power drill to mix the two together.

5.3 Torque Calculations

After running Ansys simulations and material tests, we moved forward with our torque calculations. To do so, we first used the assumed average viscosity of the material used to find the force required to press the plunger a distance of one rotation of the lead screw using the equation in Equation 1.

$$\Delta P \ = \ \frac{8\mu\widehat{m}L}{\rho\Pi R^4}$$

Equation 1: Pressure Gradient-Viscosity Equation[3]

---

[3] Woytowitz, P., slide 21

The pressure can be equated to the Force using $F = \frac{P}{A}$. This force value is then substituted into the translational work equation in Equation 2 to get the work done in the linear space. This force multiplied by 1/20th of an inch gives us the translational work required to move the plunger one rotation.

$$Work_{Translational} = Force * Distance$$

$$Work_{Rotational} = Torque * \Theta$$

Equation 2: Translational and Rotational Work Equations[4]

Since the motor coupler connects the motor shaft to the lead screw, the rotational and translational work of this system are equal. Setting the derived work equal to the second equation in Equation 2, we can find the torque required to turn the lead screw one full rotation, plugging in 2Π for θ.

---

[4] Nave, R., "Rotational Kinetic Energy."

$$\Delta P = \frac{8\mu \hat{m} L}{\rho \Pi R^4}$$

$$\Delta P = \frac{8(328 Pa.s)*(0.1 m^2/s)(0.00127m)}{(2434 kg/m^3)\Pi(0.22225m)^4} = 104.7 \; Pa$$

$$20 \; rotations = 1 \; in$$

$$1 in = 0.0254m$$

$$0.0254m/20rot = 0.00127m/rot$$

$$Density: Range \; between \; 2 \; g/cm^3 and \; 3g/cm^3$$

$$Since \; 43.4\% \; water \; content: 0.43.4*1+2 = 2.434 \; g/cm^3$$

$$2.434g/cm^3 = 2434kg/m^3$$

$$1.75in/2 = 0.875in = 0.022225m$$

$$F = \frac{P}{A} = \frac{104.7 \; Pa}{\Pi(0.022225m)^2} = 674.7 \; N$$

$$Work_{Translational} = Force * Distance$$

$$Work_{Rotational} = Torque * \Theta$$

$$Work_{Translational} = 674.7N(0.00127m) = 0.85 \; J$$

$$Work_{Translational} = Work_{rotational}$$

$$(0.85 \; J) = Torque(2\Pi)$$

$$1.33 \; Nm = Torque$$

FOS Considerations:
- Static Friction
- Clogs
- Small Long Tubing Transition
- Nozzle Outlet Transition

Chosen FOC: 3.4

Motor Holding Torque: $1.33 * 3.4 = 4.522 \; Nm$

Figure 29: Holding Torque Calculation[4]

Finally, we were able to determine the holding torque required of the stepper motor of choice. Using this value, multiplied by a generous factor of safety to accommodate for clumps in the

material, we determined that we needed a NEMA 34, a high strength stepper motor. The numerical calculation work can be seen above in Figure 29. It should be noted that the material properties used for the calculations were derived from the table in Appendix II. This scholarly journal helped with our understanding of the viscosity of clay with different water percentages.
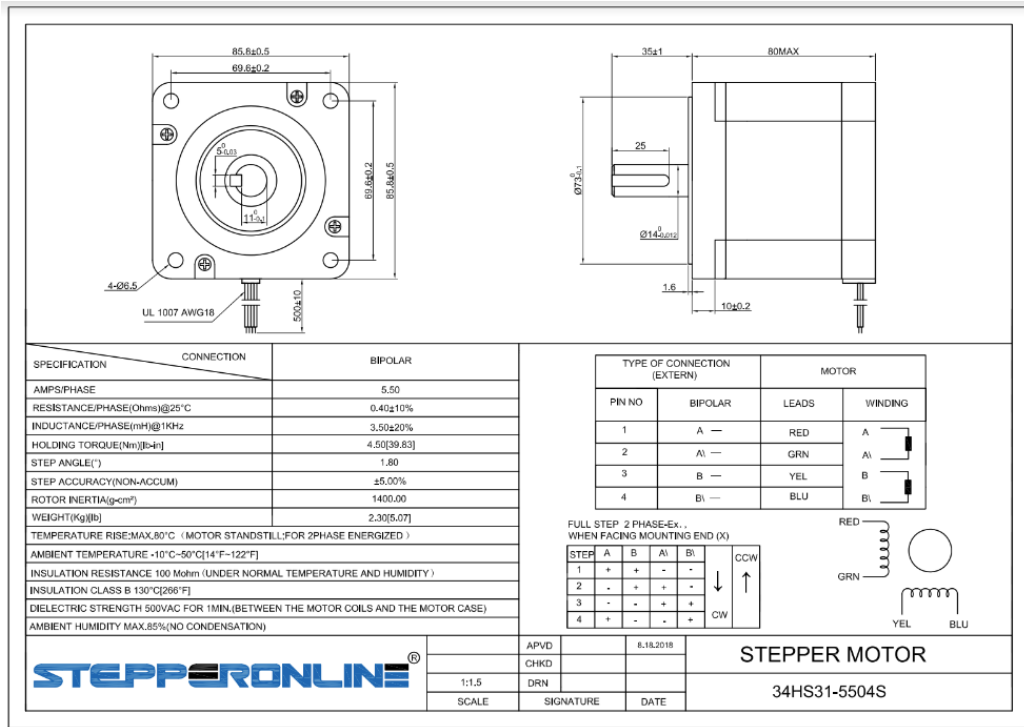
Figure 30: NEMA 34 Motor Specs

Figure 30, pictured above, displays the motor specs of our chosen NEMA 34 stepper motor. Its max hold torque rating is 4.5 Nm which matches our desired torque rating within a hundredth of a Nm.

Chapter 6: Electronics

Selecting the correct electrical components was an important part of determining the success of our system from the beginning. We wanted to ensure that we could provide adequate pressure to the chamber, while the robotic arm we used was not only cost effective but also precise with its movements. In this chapter of our thesis we will dive into the important electrical components used in our system, and the importance each component serves in helping us achieve our goal of extruding highly viscous materials.

6.1 Electrical Setup

The electrical setup that we built includes seven major components: the Rotrics AIO desktop arm (Dexarm), a DM556 motor driver, a Nema 34 stepper motor, a laptop, an Arduino Mega2560, and a large red button. Our schematic for connecting these components is shown below in Figure 31.
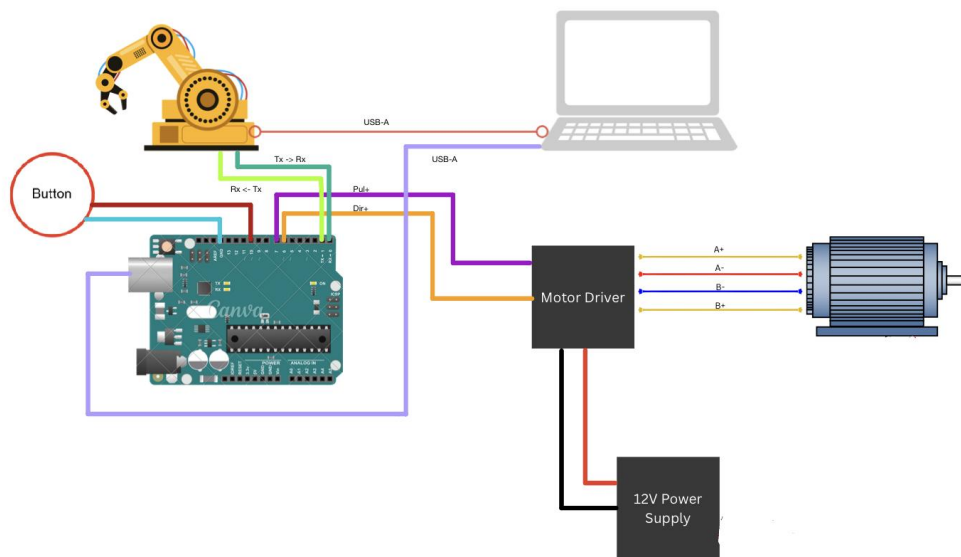
Figure 31: Electrical Layout of Components

In this electrical setup, a laptop serves as the central control unit, providing movement commands for the Dexarm robotic arm and powering the Arduino microcontroller. The Dexarm, on the other hand, has its own external power supply, ensuring it has sufficient power to operate. The Dexarm and Arduino are connected through their integrated Tx (transmit) and Rx (receive) pins, enabling communication between the two devices. To control the movement of the motors in the Dexarm, a motor driver is used. The motor driver receives pulses from the Arduino, which

acts as a signal to indicate how the motors should move. These pulses can be in the form of specific instructions or commands that dictate the speed, direction, and position of the motors. The motor driver, in turn, takes these signals and regulates the power supply to the motors accordingly, facilitating the desired movement. The motor driver requires its own power supply, nominally operating at 12V. This dedicated power supply ensures that the motors receive the necessary electrical current to function optimally and generate the required torque. Additionally, a red button is integrated into the setup. This button is connected to a communication pin and a ground pin on the Arduino. When the button is pressed, it creates a circuit connection between the communication pin and the ground pin, effectively signaling the Arduino.

6.2 Rotrics AIO Desktop Arm (Dexarm)

The Rotrics AIO Desktop arm became an ideal choice for our project due mainly to its low cost, making it an attractive option for budget-constrained projects. Despite its affordability, the arm does not compromise on accuracy. With high-precision stepper motors and a robust mechanical structure, the Rotrics AIO ensures precise and consistent movements, crucial for achieving quality prints with viscous materials. Furthermore, the Rotrics AIO offers exceptional ease of integration, which is of paramount importance for our project's success. The arm comes with a user-friendly software interface and well-documented APIs, enabling seamless communication and control. This ease of integration allows us to focus our efforts on developing and optimizing the 3D printing process for viscous materials rather than struggling with complex integration challenges. Additionally, the built-in 3D printing capabilities of the Rotrics AIO streamline our workflow and eliminate the need for separate 3D printing equipment. This integrated approach saves us time, effort, and resources, enabling us to concentrate on exploring the intricacies of 3D printing viscous materials and pushing the boundaries of this technology.

6.3 DM556 Motor Driver and Nema 34 Stepper Motor

The selection of a NEMA 34 stepper motor and DM556 motor driver for our senior design project offers numerous advantages. Through our force calculations described in the previous chapter, we decided that the NEMA 34 provided the force that we needed to push the material through the system. The NEMA 34 motor's robust torque capabilities and precise position control make it well-suited for our project's requirements, particularly in creating the required pressure for our viscous clay material. Its larger frame size allows for increased torque output and efficient heat dissipation, ensuring optimal performance under dynamic loads. Paired with the DM556 motor driver, which offers advanced features such as micro-stepping and current control, we can achieve smooth motion, improved accuracy, and effective power management. The seamless integration and compatibility between the NEMA 34 motor and DM556 driver provide a reliable and versatile motor system that contributes significantly to the success of our

senior design project. When selecting a power supply for our motor and motor driver, we found that we needed to supply 12 volts to our motor, luckily our advisor had the power supply we needed.

6.4 Motor & Robot Arm Cohesion

For our design to function correctly, we needed to implement a way for the Dexarm and our motor to communicate with each other to coordinate when to print and when to halt. This is done entirely through Python and Arduino code on our laptop. As mentioned in the previous section, the Arduino and the Dexarm communicate through the built-in Tx and Rx pins on either device, the serial message sent between each device controls how each component interacts. Movement is entirely dictated by the user through the button and the print that is loaded onto the arm. Shown below in figure 32 is the state machine for our device:
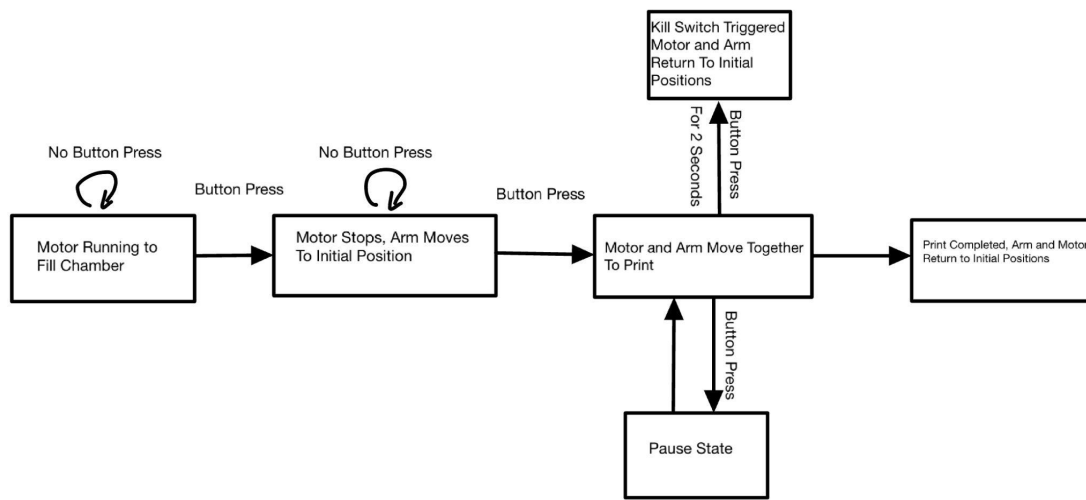
Figure 32: State Machine of Device

This is our state machine for the Python and Arduino program we built into the system. As you can see, there are 6 states. We start in the priming state where the motor turns independently to fill the tube with the material. Once the material begins to come out of the nozzle, the user presses the button and the motor stops and the arm moves to its initial position. The user then presses the button once more to begin the printing process where the motor and arm move together. From here there are 3 possible states, the print can complete and the motor stops and the arm returns to its initial position, we implemented a pause state where the user can temporarily pause and then unpause the print by pressing the button, or you can't trigger the kill switch by holding the button for 2 seconds where the program immediately stops and the arm and motor return to its initial position.

Chapter 7: System Control Software

This chapter focuses on the utilization of the Rotrics Studio software, a powerful tool that played a crucial role in our project's success. This software provides a user-friendly interface that allows us to upload our designs and customize the corresponding G-code to suit our specific requirements, specifically targeting larger layer heights and layer widths. By leveraging the capabilities of the Rotrics Studio software, we can tailor the 3D printing process to accommodate the unique characteristics of viscous materials, ensuring optimal printing results. In this section, we will delve into the features and functionalities of the Rotrics Studio software, highlighting its ability to streamline our workflow and enable precise control over the printing parameters necessary for our project's objectives.

7.1 Rotrics Software

The Rotrics Studio software serves as an indispensable tool for our project, offering a seamless workflow for uploading and customizing designs to accommodate our specific needs, such as thicker layers. This user-friendly software simplifies the process by allowing us to effortlessly upload our designs, providing an intuitive interface for modifying various printing parameters. One of its standout features is the automatic generation of G-code, which eliminates the need for manual coding. By inputting our desired layer height and width adjustments, the software intelligently generates G-code tailored to our specifications. This automated process saves us time and reduces the chances of human error, ensuring precise control over the printing process and enabling us to achieve the desired results when working with viscous materials. Shown below in figure 33 is an example print that we created on the Rotrics Studio application:
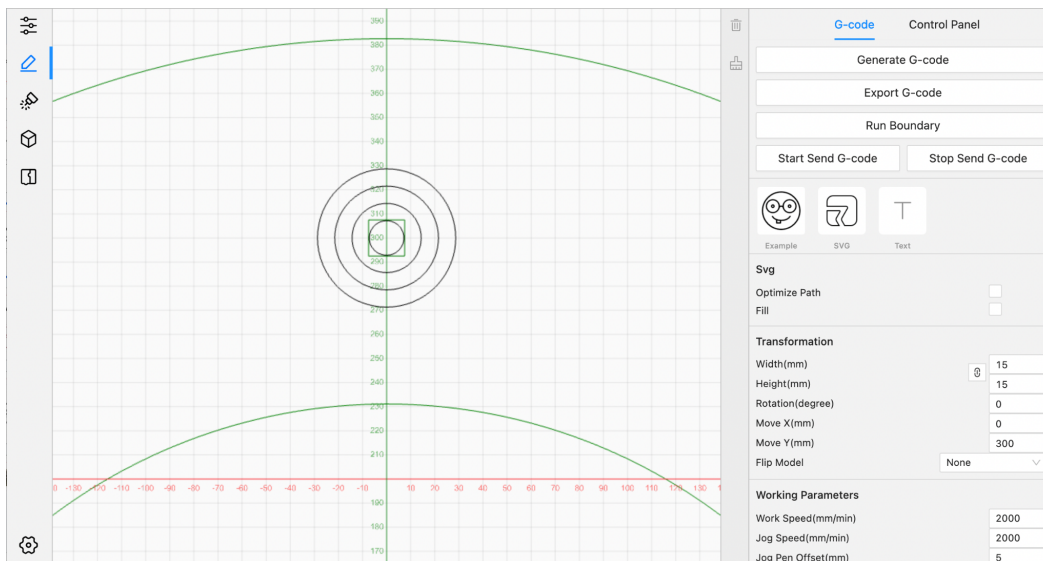
Figure 33: Rotrics Studio Application Print Example

Shown in figure 33 is how we printed the base for the bowl that we eventually printed. We would download the g-code from the application and then we would use those coordinates to construct the layers on the outside one on top of the other.

7.2 Arduino Code

The Arduino code shown below in figure 34 serves a vital role in our senior design project by controlling the motor through specific input and output pins. At the beginning of the code, the pins for the motor driver and a button are defined. The program then initializes various variables and sets up the required pin modes.

```arduino
// Define the input and output pins for the motor
int driverPUL = 7; // PUL- pin
int driverDIR = 6; // DIR- pin
int buttonPin = 10;

// Variables
int pd = 500; // Pulse Delay period
boolean setdir = LOW; // Set Direction
boolean armMoving = false;
int buttonState = LOW;
int lastButtonState = LOW;
boolean killSwitch = false;
boolean loopRunning = true;
boolean initPress = false;
boolean pause = false; // initialize pause to false
unsigned long buttonPressTime = 0;

void setup() {
      pinMode (driverPUL, OUTPUT);
      pinMode (driverDIR, OUTPUT);
      pinMode(buttonPin, INPUT_PULLUP);
      Serial.begin(115200);
}
void loop() {
      buttonState = digitalRead(buttonPin);
      if (Serial.available() > 0) {
            char incomingByte = Serial.read();
            if (incomingByte == '1') {
                  loopRunning = false;
            }
      }
      if (buttonState != lastButtonState) {
            if (buttonState == LOW) {
                  if (!initPress) {
                  // Button pressed to start loop
                        Serial.println("button pressed");
                        initPress = true;
```

```
                buttonPressTime = millis();
        }
} else {
        if (initPress) {
        // Button released
                unsigned long buttonReleaseTime = millis();//record the
                        button release time
                unsigned long buttonDuration = buttonReleaseTime -
                        buttonPressTime; // calculate the button press
                        duration
                Serial.print("Button press duration: ");
                Serial.println(buttonDuration);
                if (buttonDuration >= 2000) {
                // Button held for 2 seconds, trigger kill switch
                        Serial.println("kill switch");
                        loopRunning = false;
                        unsigned long startTimeKill = millis(); // get
                                start time
                        unsigned long elapsedTimeKill = 0;// initialize
                                elapsed time
                        digitalWrite(driverDIR, !setdir); // switch
                                direction
                        while (elapsedTimeKill < 1000) {
                                digitalWrite(driverPUL, HIGH);
                                delayMicroseconds(1000); // adjust delay time
                                        for reverse direction
                                digitalWrite(driverPUL, LOW);
                                delayMicroseconds(1000); // adjust delay time
                                        for reverse direction
                                elapsedTimeKill = millis() - startTimeKill;
                                        // update elapsed time
                        }
                } else if (pause) {
                        Serial.println("unpause"); // inverted
                        pause = false;
                } else {
                        Serial.println("pause"); // inverted
                        pause = true;
                        digitalWrite(driverDIR, !setdir); // switch
                                direction
                        unsigned long startTime = millis(); // get start
                                time
                        unsigned long elapsedTime = 0; // initialize
                                elapsed time
                        while (elapsedTime < 1000) {
                                digitalWrite(driverPUL, HIGH);
                                delayMicroseconds(1000); // adjust delay time
                                        for reverse direction
                                digitalWrite(driverPUL, LOW);
                                delayMicroseconds(1000); // adjust delay time
                                        for reverse direction
```

```
                                    elapsedTime = millis() - startTime; // update
                                        elapsed time
                                }

                                digitalWrite(driverDIR, setdir); // switch back to
                                    original direction
                        }
                        initPress = false;
                }
            }
        }
        if (loopRunning && !pause) { // inverted
                pd = map((analogRead(900)),0,1023,50,2000);
                digitalWrite(driverDIR,setdir);
                digitalWrite(driverPUL,HIGH);
                delayMicroseconds(100);
                digitalWrite(driverPUL,LOW);
                delayMicroseconds(100);
        }
        lastButtonState = buttonState;
        delay(10);
}
```

Figure 34: Arduino Code Implemented Into Our Device

In the main loop of the code, the button state is continually monitored. If a character is received from the serial interface (from the Dexarm, indicating that it is moving or not moving), and it is equal to '1' (indicating movement), the loopRunning variable is set to false, which stops the motor. When the button state changes, the code checks if the button has been pressed or released. If the button is pressed, it records the duration of the button press and performs specific actions based on the duration. If the button is held for 2 seconds, a kill switch is triggered, stopping the motor and reversing its direction for a brief period. If the button is pressed briefly, the code toggles a pause state, switching the motor direction for a short time and then returning it to the original direction.

When the loopRunning and pause conditions are met, the code reads an analog value and maps it to determine the pulse delay period (pd) for the motor. Then, it sets the motor direction, pulses the motor driver's PUL pin to generate movement, and adds appropriate delay between pulses.

Throughout the code, the button state is updated, and a small delay is included to prevent excessive processing. This Arduino code provides the necessary functionality for motor control and responsiveness to user input, facilitating the execution of our senior design project.

7.3 Python Code

This Python code snippet shown below is designed to control a Dexarm robotic arm using serial communication with an Arduino.

```python
from pydexarm import Dexarm
import serial
import time

device = Dexarm(port="/dev/cu.usbmodem305D336B34381")
ser = serial.Serial('/dev/cu.usbmodem21301', 115200, timeout=1)
ser.setDTR(False)
time.sleep(1)
ser.setDTR(True)

breakOut = False
pause = False

while not breakOut:
    if ser.in_waiting > 0:
        incoming_message = ser.readline().decode().rstrip()
        print("Received message from Arduino: {}".format(incoming_message))
        if incoming_message == 'button pressed':
            device.go_home()
            time.sleep(2)
            with open('heartfinalfr.gcode', 'r') as f:
                for l in f:
                    time.sleep(.25)
                    if l.startswith('device'):
                        exec(l)
                        print("Sent: ",l)
                        if ser.in_waiting > 0:
                            new_incoming_message = ser.readline().decode().rstrip()
                            if new_incoming_message == 'kill switch':
                                print("Kill Switch Triggered")
                                device.go_home()
                                breakOut = True
                                break
                            elif new_incoming_message == 'pause':
                                pause = True
                                while pause:
                                    time.sleep(0.01)
                                    if ser.in_waiting > 0:
                                        message_pause_handler = \
                                            ser.readline().decode().rstrip()
                                        if message_pause_handler == 'unpause':
                                            pause = False
            breakOut = True
ser.write(b'1')
```

```
ser.close()
device.close()
```

Figure 35: Python Code Implemented Into Our Device

Here is a high-level explanation of what the code does:
1. The code begins by importing the necessary libraries (pydexarm, serial, and time) and setting up the serial connection with the Arduino.
2. The code initializes the Dexarm object and opens the serial port for communication with the Arduino.
3. Within a while loop, the code continuously checks if there is any incoming data from the Arduino. If data is received, it is decoded and stored in the incoming_message variable. The received message is then printed for debugging purposes.
4. If the incoming message is 'button pressed', the Dexarm is instructed to return to its home position (device.go_home()) and wait for 2 seconds.
5. The code then opens a G-code file named 'heartfinalfr.gcode' and iterates through each line in the file. For each line, it sends the line to the Dexarm to execute the corresponding movement command. The code also checks if there is any incoming message from the Arduino during this process.
6. If the Arduino sends the message 'kill switch', the Dexarm is instructed to return to its home position, and the breakOut flag is set to exit the while loop and terminate the program.
7. If the Arduino sends the message 'pause', the pause flag is set to true, indicating a pause in the execution. The code then enters a nested while loop, continuously checking for incoming messages from the Arduino. If the message is 'unpause', the pause flag is set to false, and the code resumes normal execution.
8. Once the loop finishes iterating through the G-code file or the 'kill switch' condition is triggered, the program sends the value '1' to the Arduino via serial communication, indicating the end of the operation.
9. Finally, the serial port is closed, and the Dexarm connection is closed.

The code snippet, seen in Figure 35 demonstrates the coordination between the Dexarm robotic arm, an Arduino, and a G-code file, enabling control and execution of movement commands based on messages received from the Arduino.

Chapter 8: Testing

Once each segment of our system, Electrical and Mechanical, were independently set up to our liking, we were able to begin testing different trials of our complete system. As we have highlighted multiple times throughout this thesis, synchronization and cohesion are crucial elements to having a successful extrusion device. This chapter of the thesis will be a guide through the progression of our completed system, describing the adjustments we made from one trial to the next. We will note all of the changes made and the solutions, or problems, they provided us with.

8.1 Priming the Connection Tube

Before we began printing any full trials, we tested the priming ability of our system. Priming the tube is the process of running the motor so that the connecting tube is filled with material until the end of the nozzle. This ensures that there is material ready to print when the Dexarm begins its printing motions. Initially, when the pressure within the chamber was inconsistent, the priming time for the connection tube was around 6-8 minutes. As improvements were made to the system, that time decreased to a range of 2-3 minutes, saving the user more time overall when setting up the system for use.

Note: Adjustments made in full trials did affect the priming ability of the tube. Those will be expanded upon in future sections.

8.2 Trial 1

Once our team was successful priming the connection tube, we began running our first full trials. The first print we attempted was a single layer star pattern. As seen in Figure 36, some clay was deposited from the nozzle onto the print bed, but this trial was mostly a list of failures.
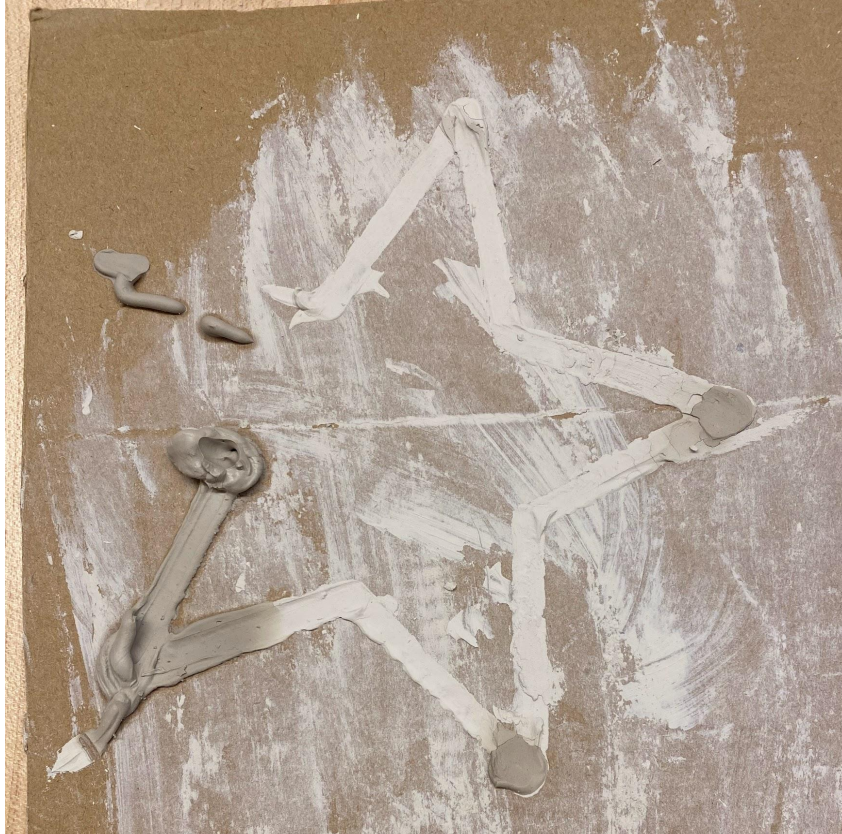
Figure 36: Trial 1 Print Bed

Figure 36 shows the first layer printed with our system. This was our first attempt at extruding any kind of material through the entire system, from the pressure chamber to the nozzle.

To start, the print flow from the nozzle was extremely inconsistent throughout the entire print. Figure 36 shows how some parts of the print are disconnected from one another due to this inconsistency issue. We determined that these inconsistencies were caused by two underlying problems which were a poor mixture of clay material and a large amount of backflow in the pressure chamber. The poorly mixed clay was filled with air bubbles and chunks of clay that caused the material coming out of the nozzle to stop extruding at certain points. The most significant problem of this trial was the backflow issue in the pressure chamber. Lots of backflow caused us to lose a lot of useful material for printing, which would have to be reloaded in front of the press if we wanted to use it, and lose pressure within the chamber. Figure 37 shows how much backflow was actually present in the chamber after simply priming the connection tube for the first time.
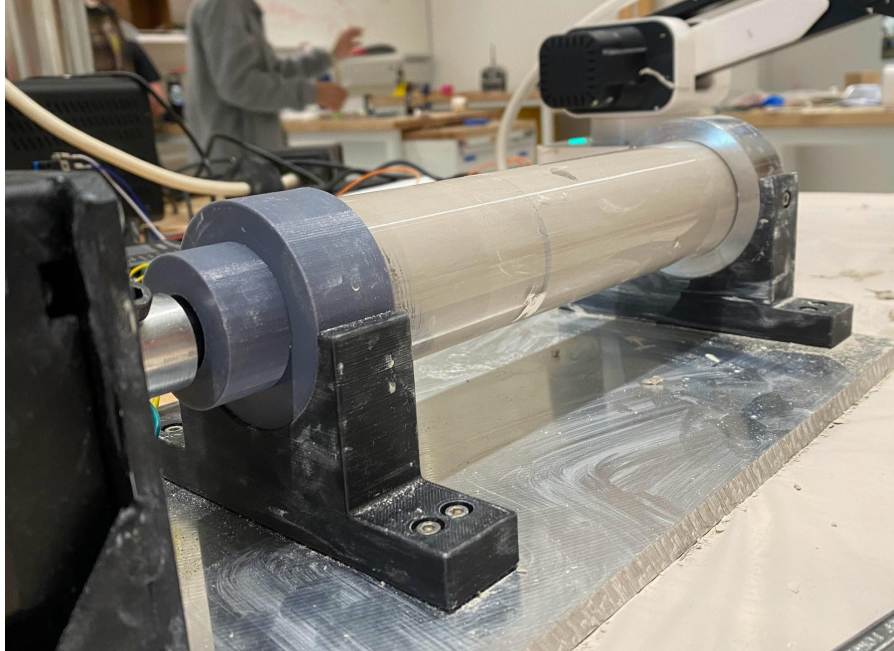
Figure 37: Backflow in Pressure Chamber

The seal between the press and the sides of the chamber was poor during this first trial.

Losing pressure resulted in the clay not being fed continuously from the pressure chamber to the connection tube and then to the nozzle. When the chamber loses pressure, no material is moved through the system for a moment so while the arm is continuing its motion, nothing proceeds to extrude from the nozzle. Due to these inconsistencies in the print, the layer height was disproportionate to our desired layer width for this trial, printing an extremely wide and short layer. Adjustments made prior to second trial testing will be discussed in the next section.

8.3 Trial 2

Prior to the second full trial, we made several adjustments to fix the print issues we faced in the first trial. The most significant change we made to our design was adding a polyurethane rod seal attachment to the press. As you can see in Figure 38, this one change virtually eliminated all of the backflow that was present in the previous trial. Since there was virtually no backflow present, higher pressure was maintained within the pressure chamber. This caused the flow rate through the connection tube and the nozzle to increase. To adjust for the increased flow rate, we chose to decrease the speed of the motor and increase the movement speed of the Dexarm from one coordinate to another to synchronize their movements for a better print.
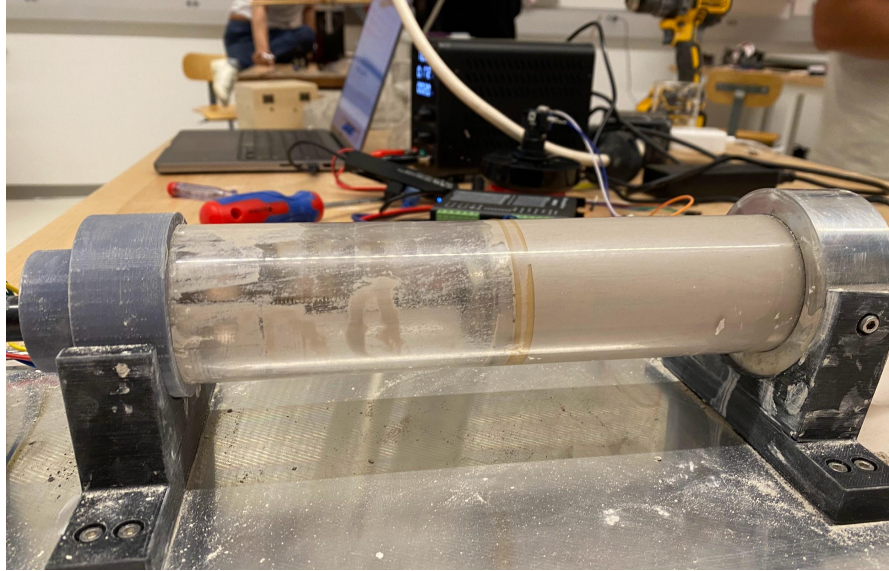
Figure 38: Polyurethane Rod Seal on Press

Figure 38 demonstrates the effectiveness of the polyurethane rod seal when added to the press.

One last additional change we made before starting this trial was to the clay material itself. We obtained a paint mixer attachment for a power drill which allowed us to mix the clay more thoroughly compared to the first trial. The speed and power from the drill made mixing large quantities of clay material easy, and it was also a more consistent process.

During the second trial, instead of printing on a cardboard cutout like in the first trial, we printed on a paint can lid. We had not really considered finding a long term paint bed at this time, so this was the flattest surface we could print on at the moment of testing. For the second trial, we also started to print multiple layers onto the print bed. Figure 39 shows how the layers were stacked one upon another, and we were all thoroughly impressed with the result.

Figure 39: Second Trial Printed Layers

Figure 39 shows the system's ability to print multiple layers during the second trial. The newly added seal helped the flow rate to be more consistent.

Due to our poor choice for a print bed, the initial layer had a hard time sticking to the print bed, but each subsequent layer printed consistently and stuck well together. We implemented two major changes to address the contact issue of the first print layer. First we obtained a few different square cuts of material from Tap Plastics to test out which one would work best for printing our clay mixture onto. Whether they were coarse or slick, we found that all of the plastic cuts worked very well in comparison to the metal paint lid. The second change we implemented was starting the print at a greater height to allow for more time to build pressure in the system. By making the Dexarm's initial position higher than before, this gave the system more time to ensure that material was ready to extrude from the nozzle. Priming ensures that material is ready, but sometimes the flow stops before the print begins due to the multiple steps that take place between priming and printing, so this additional step was a key change for this trial. An important note we would like to make is that this trial only consisted of printing wall layers. There is no flat base layer on the bottom of the structure during this trial.

8.4 Trial 3

The third and final full trial was our attempt at printing a water tight bowl. We took the successes and failures from the previous trials, putting together everything we learned, to print a thirteen layer bowl with a solid base layer. As we stated in the last section, finding a proper print bed was beneficial to our success in the third trial. These new print beds gave us better contact to our

print material, and provided us with a more level surface to print on. This increased the consistency of our print as each segment of each layer maintained similar widths and heights during the printing process.

The third trial printing the bowl was considered a success by our team. Figure 40 shows the thirteen layers we printed during this trial. We were impressed by the uniformity of all the different layers, and the clay materials ability to hold each subsequent layer.

Figure 40: Thirteen Layer Bowl

Figure 40 shows the consistency of the third trial print. We were able to print 13 layers for this trial and we were very satisfied with the quality of this print.

Although we were pleased with the results of the print, there was significant material fatigue that occurred during this trial. The front pressure chamber mount, shown in Figure 41, gives an idea of how much pressure was built up within the system when extruding material. The forward movement that occurred after the mount cracked caused some leakage to occur between the pressure chamber and the connection tube.
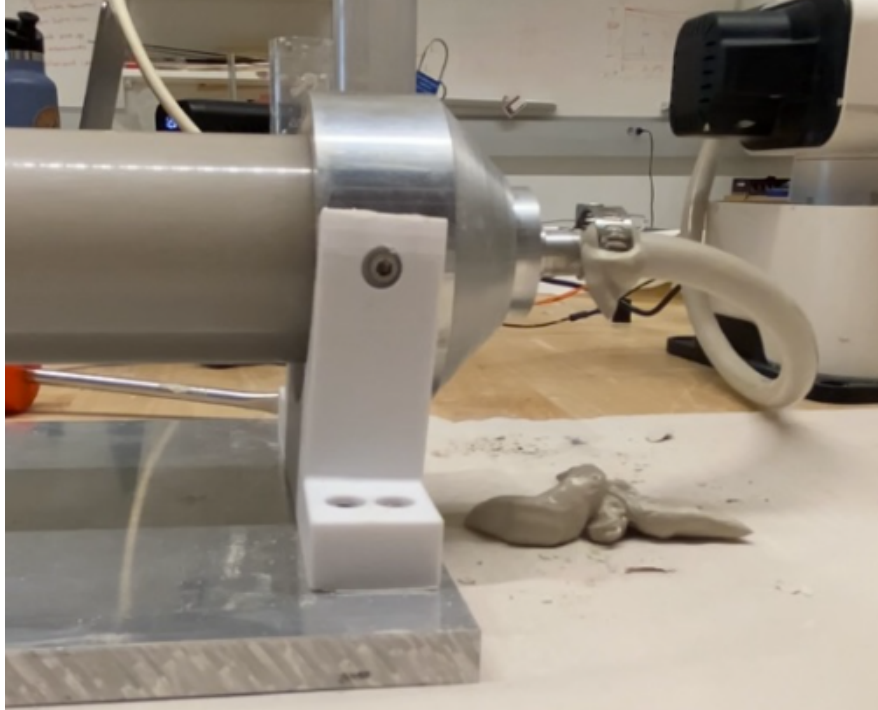
Figure 41: Cracked Front Pressure Chamber Mount

Figure 41 shows the immense amount of force applied to the front chamber mount. The mount is supposed to be perpendicular to the metal floor, but the mount struggled to hold it to that angle.

The two components were no longer properly aligned so some clay material would leak where the two were joined together. This leakage would affect the flow rate to the nozzle causing an inconsistent print. The 6-walled 3D printed PETG mount experienced significant fatigue and eventually cracked during one print. PETG is the strongest plastic material available in the Santa Clara University Maker's Lab so the fracture was surprising, indicating the significant amount of force that must have been applied. Creating a new front pressure chamber mount out of a stronger material that can withstand the force being applied would allow all of the components in the front pressure chamber and connection tube to remain properly aligned. This would prevent the leakage issues that occurred during this trial and allow for more consistent print flow.

Chapter 9: Conclusion

After fully assembling our extruder device and testing with our clay mix, our team came to various findings in regards to the quality of the extrusion, the ease of use, the efficiency of the device, as well as any bugs with the final product.

9.1 Summary

Our final prototype which includes the extruder device alongside the robotic arm and electrical hardware revealed a consistent design with respect to our initial CAD design. Our design prior to testing lacked sufficient sealing with the O-rings within the extruder device in addition to the mounting brackets which couldn't withstand the force generated by the NEMA 34 stepper motor. The PLA material used for the mounting brackets to attach the extruder to the base plate would not suffice compared to the use of aluminum alloy for the brackets. Additionally, we noticed that during the testing phase, the clay being extruded through the device would have inconsistencies, meaning that there would be more viscous portions of the clay within the device, causing the stepper motor to occasionally slip. Due to the highly viscous nature of the clay used, we attempted to add more water to the clay to ensure a more consistent extrusion. One caveat with this is that when we were to add more water to our clay mixture, the material extruded through the end nozzle would not hold up as well and would occasionally collapse under the weight of additional layers.

Another area of concern that came up was the ease of use for the extrusion system. Programming the robot arm was relatively straightforward, however, adjustments had to constantly be made to account for different layers and how quickly the material would come out of the nozzle. For instance, during one of our tests, the robot arm would move too quickly and not allow for the clay to form properly on the test surface. We would compensate for this by slowing down the robot arm, which would sometimes be too slow to the point where the material would start to smear with the nozzle. Each batch of clay used in the extruder required an adjustment for the speed of the robot arm since we were utilizing clay that we mixed by hand without precise measurement.

While we did have our fair share of missteps during our testing phase, we were able to successfully extrude a variety of bowls, stars, and hearts. Given the constraints of our extruder such as only allotting for continuous flow, we found that circular designs worked the best. Out of all the shapes we attempted, the cylindrical bowls were by far the most successful followed by the hearts we made.

Overall, our final design for the robotic arm extrusion device was successful in many ways, however, did have a fair share of challenges and issues. This is something that our team had

45

anticipated, given the level of difficulty involved with extruding highly viscous materials and going beyond that to make various designs with the extruded material.

9.2 Future Improvements

Given the time frame we had to design and complete this project, our team has created a list of potential improvements that we feel are necessary to note for those who are interested in where we believe this project could go if we had additional time to apply ourselves. The first improvement we noted was creating a system that was non-continuous. Our system relied on continuous flow for extruding the clay material. By creating a system that allows for non-continuous flow, the user would be able to print much more complex designs with the system. Our idea to accommodate for this change included creating a pressure valve that would release pressure when necessary. This would allow for precise control of the flow of material, stopping the flow when pressure is released.

The next improvement we wanted to make to our system was increasing the consistency of extrusion. While we were pleased with the prints we got from each trial, our team felt as if there was a lot of room for improvement. The clay mixture we used was prone to bubbling and clumping so using a premixed clay that has a similar viscosity to eliminate variance in testing would help streamline gathering info and obtaining consistent results. One additional improvement that we discussed earlier in Trial 3 was strengthening the front pressure chamber mount by making it out of a different material. Solving this issue would allow the system to maintain its pressure resulting in a more consistent flow rate out of the nozzle.

The final improvement we would make to the system is automating G-Code generation so it is tailored to the parameters of the premixed print material we discussed earlier. One important note we must make about this change is that it relies heavily on consistent and repeatable material flow. If possible, automating G-Code generation would enable users to be more creative with their designs and provide an easier experience for uploading new designs.

9.3 Lessons Learned

Throughout the process of determining our project scope, designing the system, fabricating and ordering parts, and finally assembling and testing, our team learned an immense amount, not only about engineering but what it means to be part of a team. We each played a unique role in the process of developing this system that, in the end, did achieve what we had set out to do. From a purely engineering perspective, we each took an idea from its beginnings to a physical system. While it did have its flaws including fatigue, leakage, and continuous flow, we were able to overcome these issues and still demonstrate our ability to complete our goals. On the mechanical design end, there were major lessons learned in terms of understanding where the

most stress will accumulate. The issue of fatigue mainly arose because we did not fully understand where the stress would be diverted to. The supporting front bracket should have been made of metal, or the system should have been designed to divert such intensive stress. As for the lessons we learned on the electrical hardware and software front, the main issue our team ran into was our lack of use of an augmented slicer. This implementation could have saved the user a lot of time by making the uploading of designs a lot easier. We had to personally customize the text files for each design, so that would make it hard for users to use any design they might want. The use of an augmented slicer, calibrated for the clay/water mixture used would make the whole system work seamlessly for anyone who would like to use it.

9.4 Cost Summary

At the beginning of this project, we set the goal of keeping this product cost effective, thus, reaching a broader audience including small businesses and hobbyists. Below, in Table 2, is our cost summary breakdown, not including the materials or parts that were gifted to us.

Table 2: Total Budget Spending Breakdown

Item	Source	Received ?	Quantity	Cost Per Item	Total Cost	Budget Left	Spent
Plaster #1 5LB	CeramicShop	Yes	1	$5.50	$5.50	$1,994.50	$5.50
Bike Pump	Amazon	Yes	1	$7.64	$7.64	$1,986.86	$13.14
Viscometer	Amazon	Yes	1	$29.00	$29.00	$1,957.86	$42.14
Beakers	Amazon	Yes	1	$18.99	$18.99	$1,938.87	$61.13
Adhesive	Amazon	Yes	1	$3.18	$3.18	$1,935.69	$64.31
Motor Board	Amazon	Yes	1	$22.99	$22.99	$1,912.70	$87.30
Motor	Amazon	Yes	1	$45.00	$45.00	$1,867.70	$132.30
Clay	CeramicShop	Yes	25	$1.06	$59.09	$1,808.61	$191.39
BreadBoards	Amazon		1	$6.99	$6.99	$1,801.62	$198.38
Grease Seal	McMaster	Yes	1	$10.92	$10.92	$1,790.70	$209.30
Threaded Nut For Lead Screw	McMaster	Yes	1	$21.49	$21.49	$1,769.21	$230.79
Lead Screw 1 ft	McMaster	Yes	1	$28.20	$28.20	$1,741.01	$258.99
Socket Head Screw	McMaster	Yes	1	$8.72	$8.72	$1,732.29	$267.71
Allen Wrenches	McMaster	Yes	1	$14.68	$14.68	$1,717.61	$282.39
Plastic Table Cloth	Amazon	Yes	1	$35.97	$35.97	$1,681.64	$318.36
Screwdriver Set	Amazon	Yes	1	$19.99	$19.99	$1,661.65	$338.35
Aprons	Amazon	Yes	1	$7.99	$7.99	$1,653.66	$346.34

DSD TECH USB to TTL Serial Adapter	Amazon	Yes	1	$12.49	$12.49	$1,641.17	$358.83
Clamping Shaft Collar	McMaster	Yes	1	$31.62	$31.62	$1,609.55	$390.45
Large O-Ring	McMaster	Yes	1	$11.27	$11.27	$1,598.28	$401.72
Silicon	McMaster	Yes	1	$20.75	$20.75	$1,577.53	$422.47
Small O-Ring	McMaster	Yes	1	$10.44	$10.44	$1,567.09	$432.91
Ball Bearing	McMaster	Yes	1	$7.35	$7.35	$1,559.74	$440.26
Motor Mount	StepperOnline	Yes	1	$7.14	$25.49	$1,534.25	$465.75
Screws Flat	McMaster	Yes	1	$7.98	$7.98	$1,526.27	$473.73
USB Hub	Amazon	Yes	1	$25.99	$25.99	$1,500.28	$499.72
M6 Motor Screws	McMaster	Yes	1	$9.76	$9.76	$1,490.52	$509.48
M6 Hex Head Screws 1mm	McMaster	Yes	1	$15.69	$9.65	$1,480.87	$519.13
Hex Nut	McMaster	Yes	1	$3.14	$3.14	$1,477.73	$522.27
Buckets	Amazon	No	1	$22.99	$22.99	$1,454.74	$545.26
Stirrers	Amazon	No	1	$10.95	$10.95	$1,443.79	$556.21
Silicon	McMaster	No	1	$17.64	$17.64	$1,426.15	$573.85
Rod Seal	McMaster	No	1	$11.40	$11.40	$1,414.75	$585.25
Bottle Brush	McMaster	No	1	4.81	$4.81	$1,409.94	$590.06
Square Oring	mcMaster	No	1	16.28	$16.28	$1,393.66	$606.34
Tube Brush	mcMaster	No	1	4.46	$4.46	$1,389.20	$610.80
Container	McMaster	No	1	14.29	$14.29	$1,374.91	$625.09

Through this chart, we can see that we spent only 31% of our budget. This means that the cost of developing this product, without including the lent materials, was only $625.09, a low price for the development of a working prototype.

In Table 3, the budget money spent is added with the items lent to us. This gives a more comprehensive breakdown of the cost of this project.

Table 3

Type	Source	Amount
Misc Budget	Misc	$625.09
Large Nozzle	Broome	$23.00
Press	Broome	$22.00

Base Plate	Broome	$50.00
Motor Coupler	Broome	$20.00
3D Print Matl	Maker's Lab	$15.00
Robot Arm	Wolfe	$300.00
Total		$1,055.09

Table 3 displays that the total cost of developing this prototype with lent and gifted items and materials came out to be $1,055.09. This is still a lower value than we expected to spend in the course of this project.

References

1. "Ansys Student Versions | Free Student Software Downloads." *Ansys*, www.ansys.com/academic/students. Accessed 13 June 2023.

2. Blake, George R. "Particle Density." *SpringerLink*, 1 Jan. 1970, link.springer.com/referenceworkentry/10.1007/978-1-4020-3995-9_406#:~:text=Densitie s%20of%20clay%20minerals%20range,than%201.5%20g%20cm%20%E2%80%933.

3. Mahajan, S P, and Muniram Budhu. "Shear Viscosity of Clays to Compute Viscous Resistance." *Shear Viscosity of Clays to Compute Viscous Resistance*, www.geocomp.com/files/papers/Shear_Viscosity_of_Clays_WEB.pdf. Accessed 7 June 2023.

4. "MC1604 1/4" Hose Barb Non-Valved Body : Colder Products Company (CPC)." *1/4" Hose Barb Non-Valved Body : Colder Products Company (CPC)*, products.cpcworldwide.com/en_US/ProductsCat/MC/MC1604. Accessed 12 June 2023.

5. Nave, R. "Rotational Kinetic Energy." *Rotational Kinetic Energy*, Aug. 2000, hyperphysics.phy-astr.gsu.edu/hbase/rke.html.

6. "Viscosity Scale." *Smooth-On*, www.smooth-on.com/page/viscosity-scale/. Accessed 12 June 2023.

7. Woytowitz, Peter. 3D Printing and Additive Manufacturing. Slide 21, file:///C:/Users/18058/Downloads/MECH171-294-ClassNotes-Wk4-Ch6.pdf. PowerPoint Presentation.

8. YoosefDoost, Arash, and William Lubitz. "Archimedes Screw Design: An Analytical Model for Rapid Estimation of Archimedes Screw Geometry." Energies, vol. 14, no. 22, 2021, p. 7812, https://doi.org/10.3390/en14227812.

9. Moretti, Francesca, et al. "Discover Our 3D Printers Solutions." Italiano, 8 Nov. 2021, www.3dwasp.com/en/.

10. "Deltabot 3D Printer: Whiteclouds." *WhiteClouds*, 5 Apr. 2023, www.whiteclouds.com/3dpedia/deltabot/.

Abstract

Abstract I

This abstract section contains a snippet from the scholarly article we originally referenced to determine the forces applied by an archimedes screw on our particular material.

upstream (Z_U) and downstream (Z_L) of the AST, where Z_U and Z_L are both measured from the same datum:
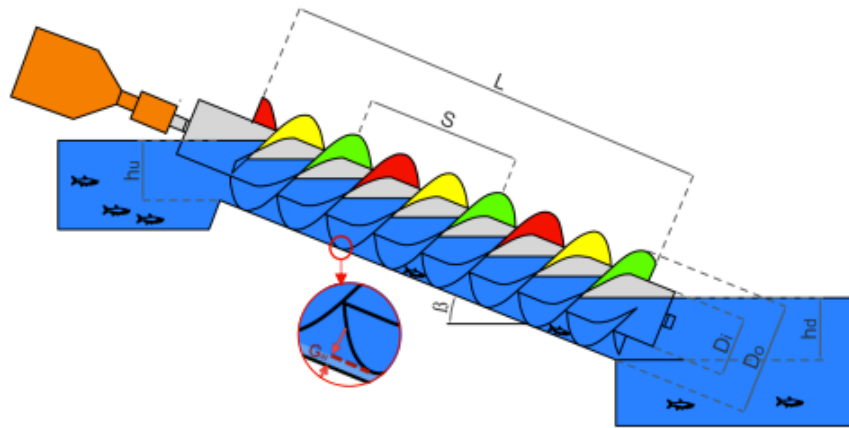
$$H = Z_U - Z_L \tag{2}$$

Figure 1. Required parameters to define the geometry of Archimedes screws [18,28].

Table 1. Required parameters to define Archimedes screws' geometry and operating variables.

Parameter		Description	Variable		Description
L	(m)	Total length of the screw	ω	(rad/s)	Rotation speed of screw *
D_O	(m)	Outer diameter	h_u	(m)	Upper (inlet) water level
D_i	(m)	Inner diameter	h_L	(m)	Lower (outlet) water level
S	(m)	Screw's pitch or period [27] (The distance along the screw axis for one complete helical plane turn)	Q	(m³/s)	Volumetric flow rate passing through the screw
N	(1)	Number of helical planed surfaces (also called blades, flights or starts [27])			
β	(rad)	Inclination Angle of the Screw			
G_w	(m)	The gap between the trough and screw.			

* Note: In the fixed speed Archimedes screws rotation speed is a constant.

The inclination angle of the Archimedes screw (β) is sometimes restricted based on slope or geometry. Considering Figure 1, for a known head the screw length (L) is:

$$L = H/\sin \beta \tag{3}$$

51

Abstract II

This abstract contains the material properties of different composition clays which we used in our calculations for the necessary torque of the motor.

Table 1. Test Data and Estimated shear strength and shear viscosity

Test	Water content (%)	h_f (mm)	h_{eq} (mm)	LI	τ_{cs} (kPa)	τ (kPa)	$\dot{\gamma}\,(\text{sec}^{-1})$	μ (Pa.s)
15C1*	35.84	9.07	5.00	0.34	38.49	57.19	3.57	516
15C2	41.93	13.77	7.46	0.70	16.71	25.64	2.90	328
15C3	43.40	17.88	9.57	0.79	9.91	15.60	2.54	253
15C4	45.51	19.44	10.51	0.91	8.39	12.93	2.44	200
15C5	43.63	18.18	9.70	0.80	9.59	15.18	2.52	253
15C6	47.43	24.55	13.13	1.03	5.26	8.29	2.17	158
5C1**	54.28	20.40	10.88	1.43	4.48	7.10	2.38	125
5C2	54.25	23.55	12.26	1.43	3.36	5.59	2.22	127
5C3	59.89	27.59	14.64	1.76	2.45	3.92	2.05	84
C1	54.25	21.23	10.79	1.43	2.69	4.70	2.34	119
C2	65.70	30.19	16.47	2.10	1.33	2.02	1.96	36
C3	58.77	18.81	10.52	1.69	3.43	4.94	2.48	55

*Tests 15C : Cone+ additional mass of 150 gm (total mass 243 gm)
**Tests 5C : Cone+ additional mass of 50 gm (total mass 143 gm)
***Test C : Cone (total mass 93 gm)

Particle density of a soil sample is actually a weighted mean value for the various kinds of minerals and humus. The measured density depends on the relative proportions of constituent minerals and humus. Densities of widely occurring minerals in the sand and silt fractions are quartz 2.65, feldspars 2.5 to 2.8, micas 2.7 to 3.3, and apatite 3.1 to 3.3 g cm^{-3} (Kretz, 1974–1975). Densities of clay minerals range from 2 to 3, but many are near 2.65 g cm^{-3}. The density of humus is usually less than 1.5 g cm^{-3}. Particle densities of samples of surface soil containing humus in fair quantities are commonly between 2.5 and...

Abstract III

This abstract is another excerpt from the scholarly article about the geometry of an archimedes screw for desired characteristics.

Extrusion

The volumetric flow equation can be obtained from the velocity equation by integrating the velocity-area product from the top to the bottom of the screw channel. Equations 5, 6, and 7 show how this integration is performed.

$$Q = \int_0^h vw\,dy \tag{5}$$

$$Q = w \int_0^h \left[\frac{Vy}{h} + \frac{(y^2 - hy)}{2\mu}\left(\frac{dP}{dz}\right) \right] dy \tag{6}$$

$$Q = \frac{Vwh}{2} - \frac{wh^3}{12\mu}\left(\frac{dP}{dz}\right) \tag{7}$$

In Equation 7 the first term of the right side is the drag flow rate and the second term is the pressure flow rate.
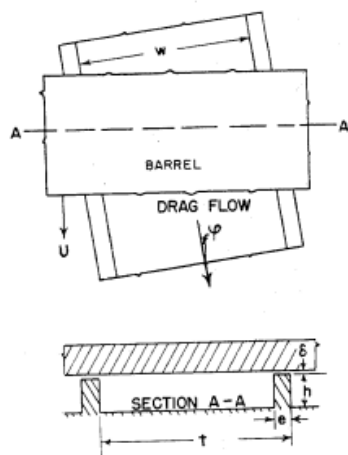

Figure 1. Diagram of Screw Channel

Equation 7 can be put into a more convenient form if the geometry of the screw thread is considered. Screws that have one or more flights in parallel may also be considered. Figure 3 shows a diagram of a double-flight screw (the simplest multiple-flight screw). If the threads from a section of the screw, which has a length equal to the lead, are unrolled from the root of the screw and laid flat they will appear as shown in bottom part of Figure 3. From the geometry of Figure 3 the following general relations can be established for screws of any number of flights.

$$V = U \cos \varphi = \pi DN \cos \varphi \tag{8}$$

$$nw = (t - ne) \cos \varphi \tag{9}$$

$$w = (t/n - e) \cos \varphi \tag{10}$$

$$dz = d\lambda/\sin \varphi \tag{11}$$

Substituting Equations 8, 10, and 11 into Equation 7 and remembering that there are n flights in parallel the basic equation of the simplified flow theory becomes

$$Q = \frac{n\pi DNh(t/n - e)\cos^2 \varphi}{2} - \frac{nh^3(t/n - e)\sin \varphi \cos \varphi}{12\mu}\left(\frac{dP}{d\lambda}\right) \tag{12}$$

Let us consider the most common special case of Equation 12—a single-flight screw whose land width is small in comparison to pitch of the screw.

As shown in Figure 3, the screw lead is related to the diameter and helix angle by the equation

$$l = \pi D \tan \varphi \tag{13}$$

Substituting Equation 13 into Equation 12 gives Equation 14 which applies to the special case of single flight screws ($n = 1$) in which the thread width is neglected.

$$Q = \frac{\pi^2 D^2 Nh \sin \varphi \cos \varphi}{2} - \frac{\pi Dh^3 \sin^2 \varphi}{12\mu}\left(\frac{dP}{d\lambda}\right) \tag{14}$$

OPERATION UNDER ISOTHERMAL CONDITIONS

Equation 12 is the basic differential equation of the simplified flow theory. Using this equation as a basis, integrated flow equations may be obtained for various special cases—for example, cases in which the screw dimensions, such as pitch or channel depth, are functions of their position along the screw. Other cases that can be calculated include certain variations of viscosity along the screw.

There follow a few of the more useful examples in which isothermal operation is assumed—that is, the temperature of the fluid is assumed to be constant at all points in the screw channel. Consequently, for Newtonian liquids the viscosity of the fluid must be constant at all points in the screw channel.
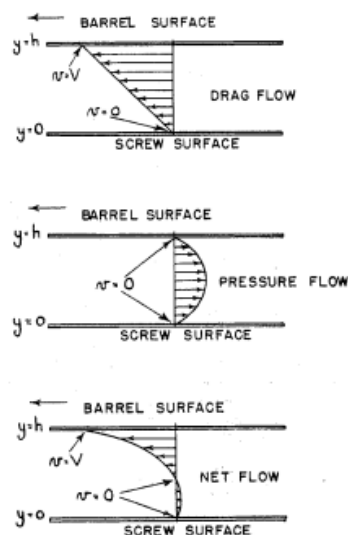

Figure 2. Velocity Distributions in Screw Channel

Extruder Flow Equations (Uniform Channel Dimensions). Here all screw dimensions are assumed to be constant over the entire length of the screw. With a uniform channel cross section and a constant viscosity the pressure gradient in the screw channel must be constant. Consequently,

$$\left(\frac{dP}{d\lambda}\right) = \left(\frac{\Delta P}{\Delta \lambda}\right) = \left(\frac{\Delta P}{L}\right) \tag{15}$$

Substituting Equation 15 into Equation 12, the flow equation becomes

May 1953   INDUSTRIAL AND ENGINEERING CHEMISTRY   975

53

Simplified Flow Theory for Screw Extruders

The flow behavior of a viscous liquid in the channel of an extruder screw is shown to be similar to the flow behavior of viscous liquids between infinite parallel plates, one of which is stationary and the other moving. Assuming Newtonian behavior of the liquid, a differential equation was derived which relates the rate of extrusion and the die pressure to the screw and die geometry and to the operating variables. Integrated flow equations are given for the special case in which the viscosity of the liquid is constant throughout the screw channel (isothermal extrusion). Equations are also given for the case in which the dimensions of the screw channel are functions of their position along the length of the screw.

J. F. CARLEY, R. S. MALLOUK, AND J. M. McKELVEY

Polychemicals Department, E. I. du Pont de Nemours & Co., Inc., Wilmington, Del.

IN THE preceding paper (*1*) of this symposium the literature pertaining to the problem of viscous flow in extruders was reviewed. In this paper the development of simplified but more useful flow equations is presented. The symbols and nomenclature used in this paper are defined in the preceding paper (*1*).

The flow mechanism of the viscous liquid in the helical channel of the screw can be better understood if one imagines that the channel be unrolled and laid out on a flat surface. Figure 1 shows this concept of the screw channel. If the lower plate, representing the screw surface, is held stationary and the upper plate, representing the barrel surface, is moved in the direction of the arrow, the relative motions will be the same as those existing in an extruder where the barrel is stationary and the screw rotates. Assuming that the liquid wets both surfaces, the motion of the barrel drags the viscous liquid along with it, while the stationary plate exerts an equal and opposite drag. The velocity of the liquid, relative to the screw, is a maximum at the barrel surface and zero at the screw surface. There is also a directional factor involved, since the channel is inclined at angle φ to the direction of motion. Therefore, in computing the flow rate in the channel we break up the velocity into two components: one of these acts directly down the channel, and the other acts at right angles to it. We call the component which acts down the channel drag velocity, and the component which acts at right angles to this transverse velocity. At the end of the channel there is generally a die or some other restriction to flow. This sets up a pressure gradient down the channel causing a flow in the reverse direction to the drag flow. We call this the pressure flow. There is one other flow that must be considered. Generally the screw does not fit perfectly inside the barrel. In other words, there is a clearance between the top of the screw threads and the barrel surface. With a pressure gradient along the screw channel, the viscous material will tend to leak through this clearance. We call this the leakage flow.

The net rate of discharge from the extruder is equal to the algebraic sum of the drag flow, the pressure flow, and the leakage flow. Equation 1 is the flow equation for the extruder, which is really a material balance made under the assumption that the liquid is incompressible.

$$Q = Q_D - Q_P - Q_L \qquad (1)$$

Neglecting the leakage flow, which is usually a small fraction of the other flows, the local fluid velocity at any point in the screw channel varies with the depth and lateral position of the point. This two-dimensional velocity distribution gives rise to Equation 2.

$$\frac{\partial^2 v}{\partial x^2} + \frac{\partial^2 v}{\partial y^2} = \frac{1}{\mu}\left(\frac{dP}{dz}\right) \qquad (2)$$

This equation is the general equation of flow for Newtonian liquids. Its derivation can be found in most books on the mechanics of viscous flow—for example (*2*).

In the preceding paper, solutions of this partial differential equation were presented. However, the resulting flow equations were complicated and difficult to manipulate mathematically. These flow equations can be greatly simplified if the assumption is made that the effect of the channel walls on the velocity distribution is negligible. In other words, the simplification is made by assuming that the special case of infinite parallel plates is applicable to the problem. This gives us a one-dimensional velocity distribution. The error caused by this approximation is quite small for shallow screw channels. When the ratio of channel width to depth is ten or larger the error will be less than 10%. Most of the screws that are used for plastics extrusion fall into this category, and consequently the simplified flow equations are very valuable for practical design work and many other applications.

DERIVATION OF SIMPLIFIED FLOW THEORY

The differential equation for the one-dimensional velocity distribution is obtained from Equation 2 by setting the second derivative of velocity with respect to x equal to zero. Equation 2 then reduces to

$$\frac{d^2 v}{dy^2} = \frac{1}{\mu}\left(\frac{dP}{dz}\right) \qquad (3)$$

By integrating Equation 3 twice, Equation 4, which gives the distribution at any point in the extruder channel, is obtained.

$$v = \frac{Vy}{h} + \frac{(y^2 - hy)}{2\mu}\left(\frac{dP}{dz}\right) \qquad (4)$$

The constants of integration were evaluated from the boundary conditions. At the barrel surface where $y = h$, the fluid velocity, relative to the screw, is V, and at the root of the screw where $y = 0$, the fluid velocity is zero.

The first term of the right side of Equation 4 is the drag flow velocity and the second term is the pressure flow velocity. The diagrams in Figure 2 show the velocity profiles of these flows. In drag flow the velocity varies linearly across the depth of the channel, while in pressure flow the familiar parabolic distribution is obtained. The addition of these two flows gives the net velocity at each point. It should be remembered that these are the profiles that would be seen on planes parallel to the axis of the screw channel. On the perpendicular planes, only the transverse velocity components, which are essentially closed circular paths, would be seen. The transverse flow is important when mixing and heat transfer in extruders are considered.